University Department of Orthopedics, Vienna, Austria

Magnetic resonance knee arthrography

Enhanced contrast by gadolinium complex in the rabbit and in humans

A. Engel

With cooperation of

P. Hajek, J. Kramer
MR-Institute, University of Vienna

G. Hamilton
Experimental Surgery Group at the University Department of Surgery I, Vienna

C. Oesterreicher
Institute of General and Experimental Pathology, Vienna

F. Lintner
Institute of Pathological Anatomy, Vienna

W. Clauss
Department for Monomer Radiologic Diagnostics, Schering Corporation, Berlin

ACTA ORTHOPAEDICA SCANDINAVICA SUPPLEMENTUM NO. 240, VOL. 61. 1990

MUNKSGAARD · COPENHAGEN

Printed in Sweden
Ortonova
Wallin & Dalholm
Lund 1990

To Barbara, my wife,

I am grateful for her doing the proofreading of my manuscript and in particular for her indulgence with respect to my work—without which I would have never been able to constantly keep my mind on magnetic resonance arthrography.

A. Engel

Contents

Introduction

Magnetic resonance imaging (MRI) has gained increasing importance as a diagnostic instrument in orthopaedics.

The possiblity to visualize diseases of the musculoskeletal system such as tumors, osteomyelitis, osteonecrosis, and disorders of the bone marrow and of the joints has given access to new information aiding in the decision between surgical and conservative management. The key to joint diagnostics, the evaluation of hyaline articular cartilage, has however not been touched sufficiently by this development. For the great hopes which magnetic resonance imaging had initially raised with respect to cartilage diagnostics were largely disappointed. The main problem turned out to be the determination of the cartilage surface and the thickness of the cartilage in the MRI image. Furthermore, the diagnosis of ligament and meniscus lesions as well as of pathological changes of the synovia also had its limitations. This was especially the case with small and partial lesions. The use of surface coils and units with higher field strengths along with gradient echo sequences took us one step further as far as local resolution is concerned.

The delineation of the hyaline cartilage against the joint space however remained unsatisfactory and with it the determination of the thickness of the cartilage and the exact size of the defect and ultimately also the correlation of the signal changes with the pathological stages of the cartilage.

The clinical relevance in diagnostics, in answering questions of detail and in the follow-up was thus only limited.

New possibilities only arrived with the development of an MRI contrast agent. The idea was to apply the contrast agent intraarticularly to delineate the hyaline cartilage. Subsequently, the following issues had to be settled:

1. Does the intraarticular application of an MRI contrast agent cause negative reactions in the hyaline cartilage and/or the synovia?

2. Can the noninvasive procedure of magnetic resonance imaging achieve the necessary improvement in the imaging quality with the intraarticular and thus invasive application of a contrast agent?

3. Is the improvement sufficient to provide answers to clinically relevant questions?

I. Principles

Justification for the use of a contrast medium

The attempt to visualize the hyaline cartilage by means of magnetic resonance imaging (MRI) represents a challenge to this technique. Comparisons of measurements of the thickness of the cartilage by MRI and by visual inspection of the cartilage, or by MRI and examination of histologic sections of the cartilage, are conspicuous by their absence.

For the entire hyaline cartilage system, assessment of the cartilage surface by MRI is necessary both for the analysis of pathologic changes (cartilage defects) and so that the MRI assessment can be compared with the findings at operation. The findings obtained by MRI are hardly comparable, however, because different machines with field strengths of from 0.15–1.5 Tesla, with different sequences (TI, T2 and gradient echo) have been used, and because of the nonhomogenous nature of the material investigated—human cartilage in vivo and in vitro, or animal cartilage [49, 7].

The statements made range from: "Articular cartilage is easily visualized in contrast to the neighbouring low-intensity cortical bone and menisci" [52], through the laconic observation: "... it also allows direct visualization of the articular cartilage..." [35] to "It is not possible to distinguish between cortical bone and cartilage" [47]. Other authors avoid the cartilage problem altogether, by not dealing with its assessment [23, 41, 6, 51]. Where a description of the hyaline cartilage is given, the emphasis varies so that attention is focused only on the cartilage surface, the thickness of the cartilage, the boundary between subchondral bone and cartilage, or the behaviour of the signal within the cartilage. Buckwalter et al. [8] could detect defects as small as 1 mm, and Wojtys et al. [79] from 3 mm upward in a cadaver study using 0.35 Tesla. Other authors, however, have observed that small superficial defects can hardly be diagnosed, if at all [80, 72, 74, 58]. It is not until a chondromalacia stage II is reached [69] that 100 percent agreement is reported [74, 80].

Almost all authors agree that a joint effusion makes it easier to assess the hyaline cartilage, and in some cases first makes this possible [39, 79, 1, 2, 7, 52]. The term "arthrogram effect" is used [80].

Table 1.1. T1- and T2-relaxation times (msec) of articular cartilage, meniscus, and different MR-contrast media. Relaxation time, *SD*

Agent	T1		T2	
Vital cartilage	1017	*217*	36	*6*
Vital meniscus	1124	*146*	30	*5*
Cadaver cartilage	455	*108*	46	*8*
Cadaver meniscus	476	*93*	51	*21*
0.9% NaCl	3660	*864*	289	*69*
Urographin 60%	3510	*720*	310	*72*
Gd-DTPA (1 mM)	237	*42*	86	*16*
Gd-DTPA (500 µM)	357	*75*	112	*16*
Gd-DTPA (100 µM)	2313	*462*	152	*26*
Albumin 24%	661	*125*	45	*8*
Albumin 12%	1476	*170*	50	*7*
Albumin 0.1%	3730	*852*	101	*23*

This arthrogram effect, whether caused by a joint effusion or by an iatrogenically-induced effusion [49, 52], formed the basis for the development of MR-arthrography.

In an earlier study [31] the signal behaviour and also the T1 and T2 relaxation times of articular cartilage, meniscus and ligaments were determined and compared with those of intraarticular blood and synovial fluid containing different amounts of albumin (24% w/v, 12% w/v, 1% w.v; Table 1.1). Sodium chloride (0.9% w/v), Urografin (60%), air and Gd-DTPA (Magnevist®, Schering, FRG) were also studied in the same way. Out of the different albumin solution concentrations, the one with 12% w/v showed the clearest differentiation from articular cartilage on T1-weighted images (Figure 1.1). Such high albumin concentrations seem to be possible when severe arthritis is present [38]. Urografin 60% and the 0.9%-NaCl-solution showed equivalent signal behaviour, but inadequate contrast. Intraarticular air yielded excellent contrast, especially of the surrounding structures. The accurate recognition of details was limited, however, because of the formation of numerous bubbles. Fresh intraarticular blood yielded inadequate contrast. Thus, except with severe arthritis the various pathological knee joint effusions that may occur

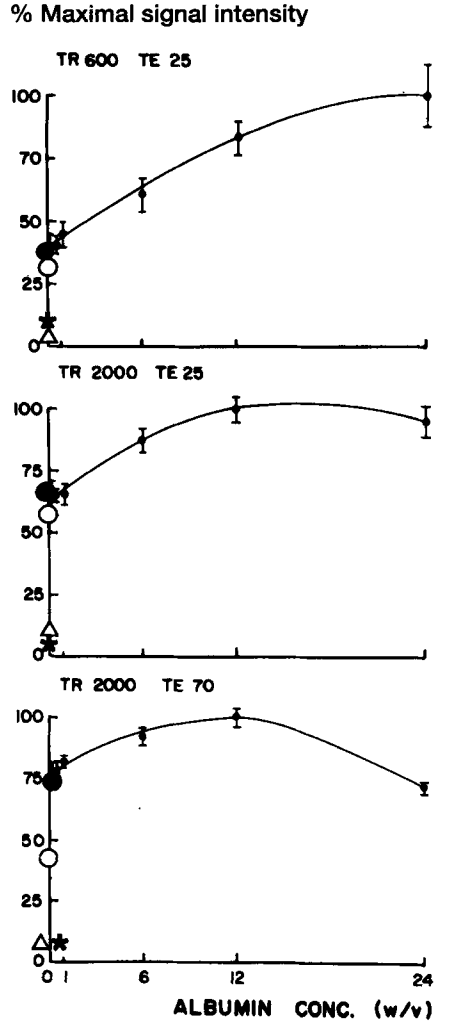

Figure 1.1. Relationship between percentage of maximum signal intensity and various concentrations of human serum albumin in 0.9% (w/v) saline for three different imaging sequences. 100% is defined as highest signal intensity for each specific imaging sequence. For comparison, relative signal intensities of cartilage, meniscus, ligaments, and 0.9% (w/v) saline are plotted on abscissa. Each point represents arithmetic mean of five measurements ± 1SD. Flattening of the curves and decrease in signal intensity for concentrations above 12% (w/v) result from increasing T2 effect [31].
○ cartilage, △ meniscus, * ligament, and ● saline.

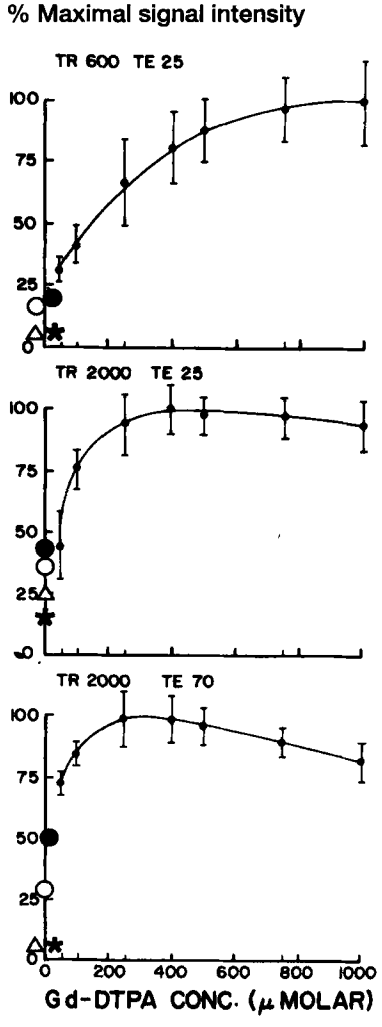

Figure 1.2. Percentage of maximum signal intensity of various solutions of Gd-DTPA-dimeglumine in 0.9% (w/v) saline for different imaging sequences. Definitions as in Figure 1.1. [31].

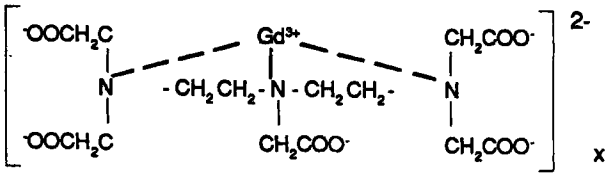

Figure 1.3. Gadopentetic acid dimeglumine salt.

Table 1.2. Properties of Magnevist® contrast medium

Concentration	(mg/mL)	469
	(mol/L)	0.5
Content per 20 mL vial	(g)	9.4
Osmolarity at 37°C	(osm/L soln.)	1.44
Osmolality at 37°C	(osm/kg H_2O)	1.96
Osmotic pressure at 37°C	(atm)	49.8
	(MPa)	5.06
Density	at 20°C (kg/L)	1.210
	at 37°C (kg/L)	1.195
Viscosity (mPa x s bzw. cP)	at 20°C	4.9
	at 37°C	2.9
pH		6.5–8.0

do not represent an ideal biological contrast medium for MRI. However, the ideal conditions were achieved with Gd-DTPA, in that there was excellent contrast in relation to all articular structures in T1-weighted images (Figure 1.2).

Chemistry of the contrast medium and the current indications for its use

The contrast medium used for MR-arthrography is a gadolinium complex with diethylenetriamine pentaacetic acid, which is supplied in the form of the dimethylglucamine salt (Magnevist®, Schering, FRG) (Figure 1.3). Gadolinium itself is an element of the rare earth group. As such, free Gd^{3+} accumulates in the liver and the spleen and is toxic. It was therefore necessary for gadolinium to be bound to a chelate complex (dimeglumine gadopentetate) with a very high stability constant of 10/22.5 (25°. 0.1 M), which is higher than that of the stable Gd-EDTA complex (stability constant = 10/17.3), before it could be used as a contrast medium (Table 1.2).

Its function as an MRI contrast medium is determined by the physical property of the gadolinium atom, since this carries 7 unpaired electrons and therefore is strongly paramagnetic. This property affects the relaxation time in an aqueous medium, which is decisive for the imaging. There is a reciprocal relationship between the concentration of the paramagnetic substance and the 1/2-relaxation time: the higher the concentration of the Gd-DTPA, the shorter is the resulting relaxation time.

Measurements of the signal intensity showed that with increasing concentrations intensity increased in T1-weighted images, but only up to a concentration of 1 mmol/L [22] (Figure 1.4). At higher concentrations there was actually a decrease. This is due to the increasing T2-effect (decay of the signal).

Experimental and laboratory investigations are available on the testing of the contrast medium Gd-DTPA for clinical use, all of which report good tolerance with minimal side-effects. The preparation was therefore licensed by the Medicines Committee in Austria in 1984 (Running No. 225).

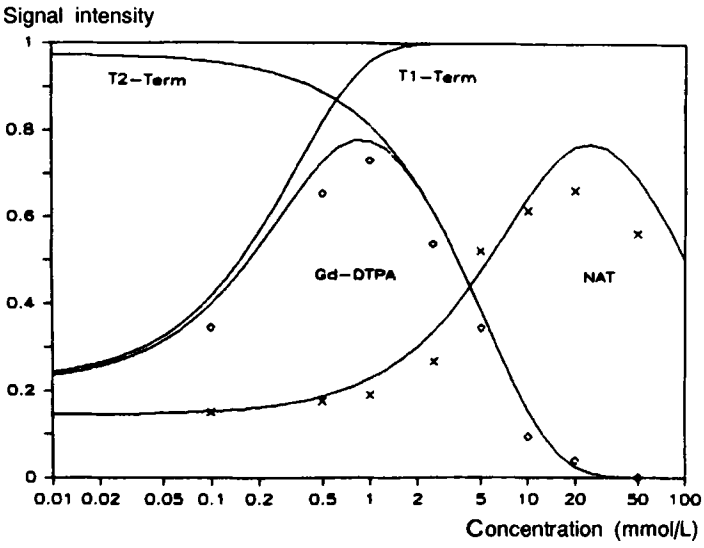

Figure 1.4. Calculated signal intensity (lines, 10 MHz, 37 °C) and measurements (points, 15 MHz, 23 °C) depending on the concentration of Gd-DTPA and NAT in water and also the calculated T1- and T2-term for Gd-DTPA in spin-echo images (SE 0.5/28). ◇ Gd (15 MHz) and × NAT (15 MHz). Reproduced from Gadian et al. 1985 [22].

Fundamental studies of intraarticular use

Uptake of Gd by rabbit cartilage in vitro

To determine whether the contrast medium—after being incorporated into the hyaline articular cartilage—was stored in the chondrocytes, uptake experiments were carried out in vitro on rabbit knee-joint cartilage with radioactive 153Gd or with a radioactive 153Gd-DTPA-BSA-complex, and an exchange experiment was performed using radioactive 153Gd versus Gd-DTPA. The uptake of 153Gd into cells was investigated with neuroblastoma cells, connective-tissue cells and chondrocytes.

Uptake of 153Gd by the articular cartilage

The kinetics of the uptake of free 153Gd by the cartilage in vitro was determined for incubation periods of 5 h and 24 h. In each experiment 6 knee preparations were incubated in 10 mL of tissue-culture medium each (RPMI-1640/HEPES-medium with 10% foetal calves' serum, 20 mM glutamine and 75 mcg/mL of gentamycin) at room temperature with 171 kBq of 153Gd. At the end of the incubation period, the cartilage preparations were washed three times with phosphate-buffered saline (PBS) and removed in three layers. After the wet weight of the pieces had been determined, the radioactivity taken up was measured in a gamma counter (Kontron, Zurich, Switzerland; counting over the entire range). The total activity in the supernatant corresponded to about 500,000 cpm/mL medium. The amount of 153Gd taken up was expressed as a percentage of the total radioactivity in the supernatant at the start of the incubation (Table 1.3).

Uptake of 153Gd-DTPA-BSA by the cartilage

The compounds of BSA (bovine serum albumin), DTPA (diethylenetriamine pentaacetic acid) and Gd were prepared by the method described by Hnatovich et al. [36]. BSA (1 mg) was conjugated with DTPA, free DTPA was removed by gel filtration in Sephadex PD10 columns (Pharmacia, Uppsala, Sweden) and the complex was incubated with 370 kBq 153Gd. Free Gd was removed by column chromatography and the 153Gd-DTPA-BSA-complex (molecular weight 70,000 Daltons) was incubated again, in the medium with articular cartilage (24 and 8 h) as described for 153Gd.

In this in vitro experiment, 153Gd, in the form of the large protein complex, was taken up very slowly into the articular cartilage. Only one fourth of the original radioactivity of the medium was found in the innermost layer after 48 h (Table 1.4).

Table 1.3. Uptake (percentage of the total radioactivity in the supernatant at the start of the incubation) of 153Gd by the articular cartilage (n 6). Mean, *SD*

Incubation period	5 h		24 h	
Outer layer	60	*7.8*	194	*22*
Middle layer	39	*5.4*	111	*14*
Inner layer	13	*3.7*	113	*18*

Table 1.4. Uptake (percentage of the total radioactivity in the supernatant at the start of the incubation) of 153Gd-DTPA-BSA by hyaline cartilage (n 5). Mean, *SD*

Incubation period	24 h		48 h	
Outer layer	7.7	*3.3*	44	*4.2*
Middle layer	11.1	*2.8*	39	*7.9*
Inner layer	2.1	*1.9*	24	*4.6*

Table 1.5. Exchange experiment. Uptake of 153Gd (cpm/mg wet weight) after 24 h pretreatment with Gd-DTPA (n 4). Mean, *SD*

Pretreatment	No		Yes	
Outer layer	310	*170*	218	*120*
Middle layer	196	*80*	51	*7*
Inner layer	156	*91*	100	*6.4*

Exchange experiment Gd-DTPA versus 153Gd

The metglobin complex of the gadolinium-DTPA was not available in radioactively labelled form for the experiments. Investigations were therefore carried out into the effects of preliminary incubation of the joint preparations with gadolinium-DTPA (24 h; 1: 150 dilution in tissue culture medium) on the subsequent uptake of 153Gd (24 h incubation). (Four preparations in each case; values in cpm 153Gd/mg wet weight).

No differences could be demonstrated in the outer layer of the articular cartilage because of the great standard deviations. In the middle layer, pretreatment with gadolinium-DTPA led to a 75% reduction in the subsequent uptake of radioactive Gd. The metglobin complex therefore reached the middle layer of the articular cartilage within the incubation period. However, it did not reach the innermost layer (Table 1.5).

Uptake of 153Gd by isolated cells

1) Neuroblastoma cells in tissue culture. SK-N-MC neuroblastoma cells from a human-tumour-cell bank (10 x 10 cells in 5 mL of tissue-culture medium) were incubated for 24 h with 74 kBq 153Gd under tissue-culture conditions. After the cells had been washed twice with PBS, the uptake of radioactivity was measured. Approximately 6% of the 153Gd in the medium had been taken up in this time.

2) Connective tissue cells and chondrocytes. Four articular cartilage preparations were labelled with free 153Gd for 48 h as described above, then washed twice with PBS. The connective tissue was then incubated for 7 h at 37 °C with 1 unit of collagenase (Type VS; Sigma, St Louis, USA) in medium, after which the radioactivity taken up was measured. Out of the total activity present (460,000 ± 44,700 cpm) only 6.3% (28,900 ± 6,850 cpm) was taken up into the cells.

Comments

These experiments showed that gadolinium is taken up completely into the hyaline cartilage, and that this process is time-dependent. Binding to a DTPA-BSA-complex resulted in a marked reduction in the rate of incorporation. The contrast medium is similarly taken up into the cartilage matrix, but to a distinctly lesser extent, and it penetrates only to the middle third of the cartilage within 24 hours. From this it can be concluded that within the short period of time between intraarticular injection and measurement of the image data, only extremely small amounts of Gd-DTPA are taken up into the matrix as a result of the porosity of the hyaline articular cartilage. Therefore no adverse effect on the assessment of the cartilage thickness is to be expected from signal changes caused by Gd-DTPA localised in the matrix. Since degenerative articular cartilage is characterized by fissure formation or the loss of cartilage substance because of the breakdown of collagen and the destruction of chondrocytes, the uptake of Gd-DTPA into the remaining cartilage is dependent on its fluid content. Thus, Gd-DTPA can be introduced into the matrix to a greater extent in stage 1 of chondromalacia—increased fluid content—than into healthy hyaline articular cartilage. A smaller uptake of Gd-DTPA is to be expected in advanced stages of arthrosis (Stages II and III according to Ficat and Hungerford [20]) because of the reduced content of water in the matrix.

Besides the incorporation of gadolinium into the matrix, the cell investigations have shown that only 6% of the radioactive gadolinium is taken up into tumor cells and chrondrocytes. It is permissible therefore to conclude, indirectly, that the uptake of a molecular complex with a molecular weight of 550 Daltons is distinctly less than 6% or, as is more likely, that it does not penetrate the cell membrane of the chondrocyte at all. This behaviour has been demonstrated in blood cells by Weinmann et al. [77].

Demonstration of gadolinium-DTPA in cartilage and synovial membrane of the rabbit knee-joint after intraarticular administration

In vitro studies were carried out in rabbits to discover firstly whether the intraarticular administration of Gd-DTPA leads to macroscopically and histologically visible changes in the articular cartilage and synovial membrane, and secondly whether Gd-DTPA can be demonstrated in the articular cartilage.

2 mL of a 0.5-mmolar solution of Gd-DTPA-dimeglumine (pH 7.2) were injected into the right knee joint in 10 rabbits (white New Zealand rabbits, 3,000 to 4,000 g). In order to determine whether the instillation itself might have an effect on the knee-joint, 7 left knee-joints were filled with 2 mL of a 0.9% NaCl-solution. A second control group consisted of 9 untreated joints. The animals were killed after 2, 6, 24 and 72 h and after 8 days.

In the macroscopic investigation of the gadolinium group, one knee-joint showed an effusion (after 6 h) and another displayed slight hyperaemia 24 hours after the injection. The same result was obtained in the group given physiological NaCl-solution. The knee-joints of the untreated control group were normal.

In the histologic investigation, the Gd-DTPA group showed minimal focal hyperplasia of the synovial membrane in four joints (after 2, 6, 24 h and 8 days), and mononuclear-cell infiltrates in three after 6, 24 h and 8 days. The same changes were observed in two knees in the NaCl-group after 2 hours and 8 days.

The retention-time of Gd-DTPA in the articular cartilage was studied by radio-fluorescence-spectroscopy (Quantex-Ray/Micro-X 7000 Analytical Spectrometer; Kevec Corp, Foster City, California, USA). With this investigation technique, no gadolinium could be demonstrated in the individual groups after 2, 6, 24 and 72 h and 8 days.

The radio-fluorescence-spectroscopy is sufficiently selective for the demonstration of gadolinium up to a maximum of 5-molar Gd-DTPA.

The macroscopic and microscopic analyses revealed no differences between the gadolinium- and the NaCl-groups. They also showed that gadolinium is transported out of the articular cartilage again within a short space of time [33].

Demonstration of Gd-DTPA in cartilage and synovial membrane of the human knee-joint after intraarticular administration

The methods used for trace-element analysis were applied in order to detect any gadolinium, given by intraarticular administration, that might still be present in the cartilage and synovial membrane.

Method

After previous administration of the contrast medium to patients who had received a knee endoprothesis for arthrosis, pieces of cartilage were taken from two areas of the medial and lateral condyles in accordance with accepted resection practice (10 knee-joints, zones 2 and 3, for diagram see Appendix). The freeze-dried pieces of tissue were subjected to pressure decomposition by the method of Tölg (Table 1.6). The analysis of the pieces of cartilage and bone and of the synovial membranes was carried out with an inductively-coupled plasma-quadrupole mass spectrometer (ICP/MS) of the "Plasma-Quadrupol" type from the Vg/Isotopes Company. Plasma is used as the excitation source here. The advantage of this method lies in the considerably higher excitation temperature (approximately 8.000K for argon plasma) and in the fact that the plasma constituents are present not only in atomized but also largely in ionized form. Ions of all elements whose ionization energies are not higher than those of argon (15.57 eV) are formed in the argon plasma. The entire plasma-quadrupole ICP (MS-system) consists of four function-blocks: plasma production, interference, Quadrupole-mass spectrometer, and data processing.

The mass spectra obtained covered the range from 49 to 240 AMU. The measurement range below 49 AMU was not measured because the high content of mineral elements (Na, Mg, P, S, Cl, K, Ca) in this range would lead to such high measurement signals that the multiplier would be overloaded which would lead to a reduction in sensitivity during the measurement.

The masses of Br^- and I^- were not measured, since both elements require special sample preparation and measurement techniques. Calibration was carried out by means of external multi-element standard solutions.

Table 1.6. Decomposition conditions according to Tölg

Weight of tissue sample	50 mg
Amount of acid	HNO_3 700 µL
Temperature programme	6 h 160 °C
Dilution	50 g H_2O

Table 1.7. The Analytical Measurement System (AMS) was tested on standard materials with certified values (all data given in ppm dry weight)

	Bovine liver 1577 a		Animal muscle H-4		Animal bone H-5	
	NBS	AMS	IAEA	AMS	IAEA	AMS
Mn	9.9	10	0.25	0.25	–	0.7
Co	0.21	0.26	0.004	<0.05	–	0.03
Cu	158	129	4.0	3.6	–	0.4
Zn	123	109	86	80	89	88
Rb	12.5	12.7	19	19	–	0.5
Sr	0.14	0.13	–	–	96	88
Mo	3.5	4.0	0.05	0.07	–	0.2
Cd	0.44	0.46	–	–	–	–
Cs	–	–	0.12	0.13	–	–
Ba	–	–	–	–	79	75
Pb	0.14	0.10	–	–	3.1	2.8

NBS National Bureau of Standards
IAEA International Atomic Energy Agency

The analytical methods were controlled and tested with the standard materials, bovine liver (NPS bovine liver SRM No. 1577a), animal muscle (IAEA animal muscle H-E) and animal bone (IAEA animal bone H-5). The certified values of the National Bureau of Standards (NBS) and the International Atomic Energy Agency (IAEA) and the values which we obtained with the Analytical Measurement System (AMS) are summarized in Table 1.7. The recovery rate was approximately 100%.

Most of the measured trace elements lie in the range from 1 ppb to 1 ppm (1 mcg/kg to 1 mg/kg).

The lowest accurately measurable range for gadolinium was established as 0.05 ppm. Values above 0.2 ppm were classified as lying above the norm.

Results

The gadolinium concentrations measured in the different areas of the cartilage showed values which, apart from two borderline values (Cases 3 and 5) lay exclusively near the lower limit of detection (Table 1.8). No relationship was found between the time of

Table 1.8. Multielement determination using an inductively coupled plasma-quadrupole-mass spectrometer (ICP/MS) in articular cartilage and synovial membranes (ppm dry weight)

Case	Age	Sex	Period in hours i.a. inj.–op.	Medial femur		Lateral femur		Synovial membranes	Gd-DTPA/ mmol
				Zone 2	Zone 3	Zone 2	Zone 3		
1	67	f	17	< 0.05	< 0.05	< 0.05	0.05	< 0.07	1
2	83	m	18	0.09	0.09	0.09	0.09	3.4	4
3	57	m	19	0.08	0.1	0.08	< 0.05	0.06	2
4.	73	f	19	0.06	< 0.05	< 0.05	< 0.05	–	2
5	80	f	20	0.08	0.2	0.05	0.1	0.67	5
6	81	f	43	0.09	0.06	0.07	0.08	1.6	5
7	67	f	62	0.06	< 0.05	0.05	< 0.05	0.67	2
8	83	m	64	< 0.05	< 0.05	< 0.05	< 0.05	0.35	2
9	56	f	73	< 0.05	< 0.05	< 0.05	0.07	–	5
10	73	m	137	< 0.05	< 0.05	< 0.05	< 0.05	0.21	5

the intraarticular administration or the taking of the samples and the concentration of Gd-DTPA or the measured gadolinium conjugates. This underlines the fact that Gd-DTPA is eliminated very rapidly via the kidneys. Investigations have shown that after the i.v. administration of 0.1 mol Gd-DTPA/kg, 83% has already been excreted renally after 6 h; the amount 5 days after the injection is 91%. About 1% of the contrast medium is excreted via the stools [65].

The values measured in the synovial membranes were higher than those in the cartilage in all patients, especially in patients aged over 80 years (Table 1.8). Our investigations did not provide any explanation for this, but fibrosis of the capsule and altered permeability might play a role.

Influence of intraarticular administration of Gd on laboratory parameters of liver function

In order to determine whether the intraarticular administration of Gd-DTPA leads to an increase in the laboratory parameters, indicative of an hepatotoxic action, the following measurements were carried out before and a few days after the instillation of the contrast medium: the transaminases GOT (glutamate oxalacetate transaminase) and GPT (glutamate pyruvate transaminase), gamma-GT (glutamyl-transpeptidase), bilirubin, alkaline phosphatase and LDH (lactate dehydrogenase) as indicators of any possible cholestasis. The investigations were carried out in 20 patients who had received a knee endoprosthesis for severe arthrosis. Thus continuous monitoring was guaranteed, also enabling us to do laboratory checks in order to discover any change in the parameter; this was done in addition to observing increases in iron and bilirubin levels within 24 hours following intravenous Gd-DTPA application [55].

Results

The average period of time between the two determinations of the enzyme values was 7.6 (2–20) days. The values after treatment deviated slightly from normal in 7 out of the 20 patients, but with two exceptions the same values had already been found in the initial samples.

Determination of the optimal concentration of contrast medium for imaging

Concentration and signal intensity studies have shown that in T1- and T2- weighted images the signal intensity increased with increasing concentration of Gd-DTPA but only up to a concentration of 1.0 mmol/L [22] (Figure 1.4). Very high concentrations did not result in any further improvement in the signal intensity, but led rather to a decrease. In the investigations of Hajek et al. [31, 32], carried out on cadaver knee joints, 0.5 mmolar was found to be the lowest concentration that was just about adequate. However, since the amount of free synovial fluid varies, these two statements about concentration cannot be applied in vivo.

MR-sequences used

A 1.5 Tesla superconducting magnet (Magnetom 63, Siemens Co., Erlangen, FRG) was used for the MR-investigations. The imaging was carried out by means of a circular-polarised surface coil ("knee-resonator") 20 cm in diameter. Sagittal slices were produced and

were supplemented by coronal and transverse section scans in some cases.

T1-weighted spin-echo sequences. The following parameters were used:

TR 700 msec; TE 15 msec; slice thickness 3–4mm; gap between slices 0–20% of the slice thickness; image matrix 256 x 256.

T2-weighted spin-echo sequences. The following parameters were used:

TR 2500 msec; TE 15/90 msec.

Gradient echo sequences. Both a 2D and a 3D gradient technique were used for the gradient echo sequences:

Flash 2D TR 300 msec; TE 10 msec; excitation angle (alpha 135°); effective slice thickness 1–3 mm.

Flash 3D TR 30msec; TE 10 msec; excitation angle (alpha 30°–50°); effective slice thickness 1–3 mm.

Randomised study to establish the optimal concentration of contrast medium

In a randomised study on 20 patients, a Gd-DTPA solution was given by intraarticular administration in concentrations of 1, 2, 4 and 5 mmolar in vivo (decision of the Ethics Committee of the University of Vienna, 1988-04-12). Signal behaviour in relation to the articular cartilage was then determined on T1-weighted images.

In 1 and 2 mmolar solutions and occasionally also in 4 mmolar solutions, there was excellent contrast in the imaging of the articular cartilage. If a fairly large effusion was present there was excessive dilution and thus inadequate contrast with a 1 mmolar concentration of Gd-DTPA, so that the 2 mmolar solution was found to be the optimal concentration. 0.5 mmolar solution injected twice resulted in only inadequate contrast because of marked dilution phenomena. The 5 mmolar solution resulted in excessive contrast, leading to spreading of the image in the MR-tomogram. Only 2 mmolar solutions were therefore used for the subsequent investigations.

Comparison between images of the hyaline cartilage with and without contrast medium

A comparison of the published interpretations of the cartilage layers is possible only for T1-weighted images. Burk et al. [9] and Vogl et al. [76] are the only authors who say that the hyaline cartilage can be divided into two layers, the layer that adjoins the joint cavity having an intermediate signal intensity and that which adjoins the cancellous bone a low signal intensity. Each of these layers is given as 2 mm by Burk et al. [9].

In contrast to these authors, other authors [50, 52, 46, 30] correlate the zone of lower signal intensity with the subchondral bone. Adam et al. [1] is critical of this interpretation since, according to their data, anatomically the subchondral plate and the mineralised part of the cartilage taken together amount to only 0.3 mm, whereas the slices measured on the MR-image amount to 1–5 mm.

Steinbrich et al. [72] interprets the altered signal behaviour as hyperdense imaging of cartilage, which he correlates with low-signal cortical bone. Lehner et al. [47] on the other hand, distinguishes between a superficial layer of low-signal intensity and a deep layer of intermediate signal intensity.

König et al. [44] distance themself from these problems in that—in connection with the view that the hypointense signal is to be ascribed to the subchondral zone—they do not allocate the signal to any anatomical structure and points out that the imaging of the articular cartilage may perhaps be affected by chemical shifts, which cause the division into two layers. The influence of chemical shifts is also pointed out by Mink et al. [52] and Weinreb et al. [78]. But this is refuted both by Adam et al. [1], who used a 1.5 Tesla machine and Reicher et al. [60] with a 0.3 Tesla machine; neither of these authors having so far noticed any chemical shifts. In this connection, Weinreb et al. [78] observes that chemical shifts are a problem with high-field machines but not with low-field equipment, since the signal zones could be distinguished to an equal extent both in 7.5 mm and also in 2 mm slices through rotating beam gradients. From this Adam et al. [1] concludes that there is not a chemical shift artifact but rather a boundary surface artifact which is due to the cartilage/bone stratification. It is also Adam et al. [2] who describes stratification in the structure of the articular cartilage with gradient echo sequences. He distinguishes between a superficial layer of low intensity and a zone of intermediate signal intensity.

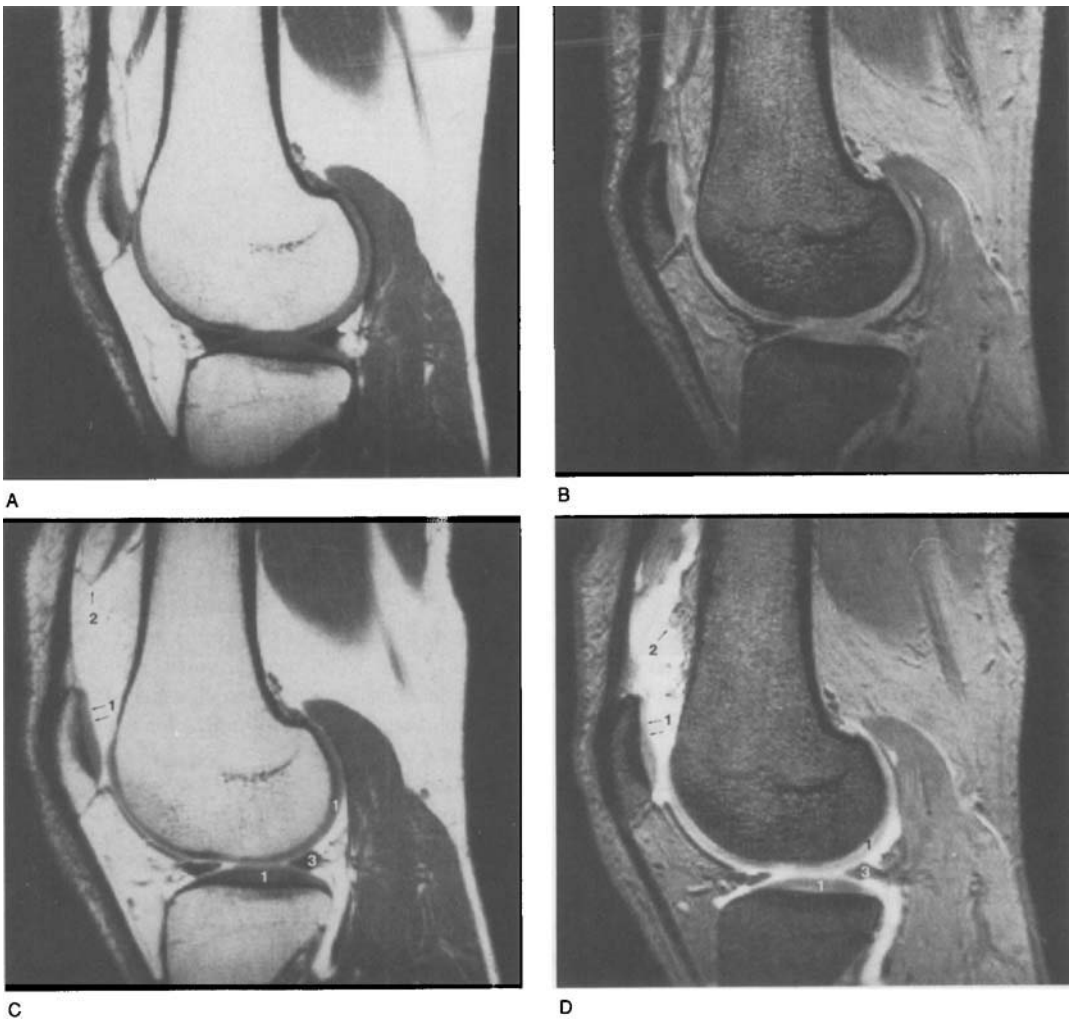

Figure 1.5. Normal hyaline articular cartilage. MRI, SE 700/15 (A and C), GE 300/10/30°, FISP-3D (B and D), normal knee joint, sagittal plane, immediately lateral to the medians.

A and B. Before the intraarticular injection of 30 mL of a 2 mmolar Gd-DTPA-solution.

C andD. After the injection (MR-arthrography).

MR-arthrography (C+D) makes accurate visualization of the cartilage surface possible and also a differentiation between the patellar, femoral and tibial articular cartilage (1). In addition the synovial surface (2) and the meniscii and their supporting attachments (3) can be assessed.

Personal assessment

On T1-weighted images, the articular cartilage is seen with intermediate signal intensity. It is not possible to assess its surface or to demarcate this from the synovial fluid.

Depending on the amount of joint effusion present, the demarcation of the articular cartilage can be achieved by means of gradient echo images. After aspiration of the effusion and administration of the contrast medium, excellent and reproducible assessment of the surface of the cartilage is obtained.

Besides an accurate assessment of the cartilage surface, the contrast medium (MR-arthrography) also makes possible the delineation of the patellar, femoral and tibial articular cartilages.

The cartilage itself, which is of intermediate signal intensity, appears to be of approximately the same thickness on T1-weighted and gradient-echo images (Figure 1.5.).

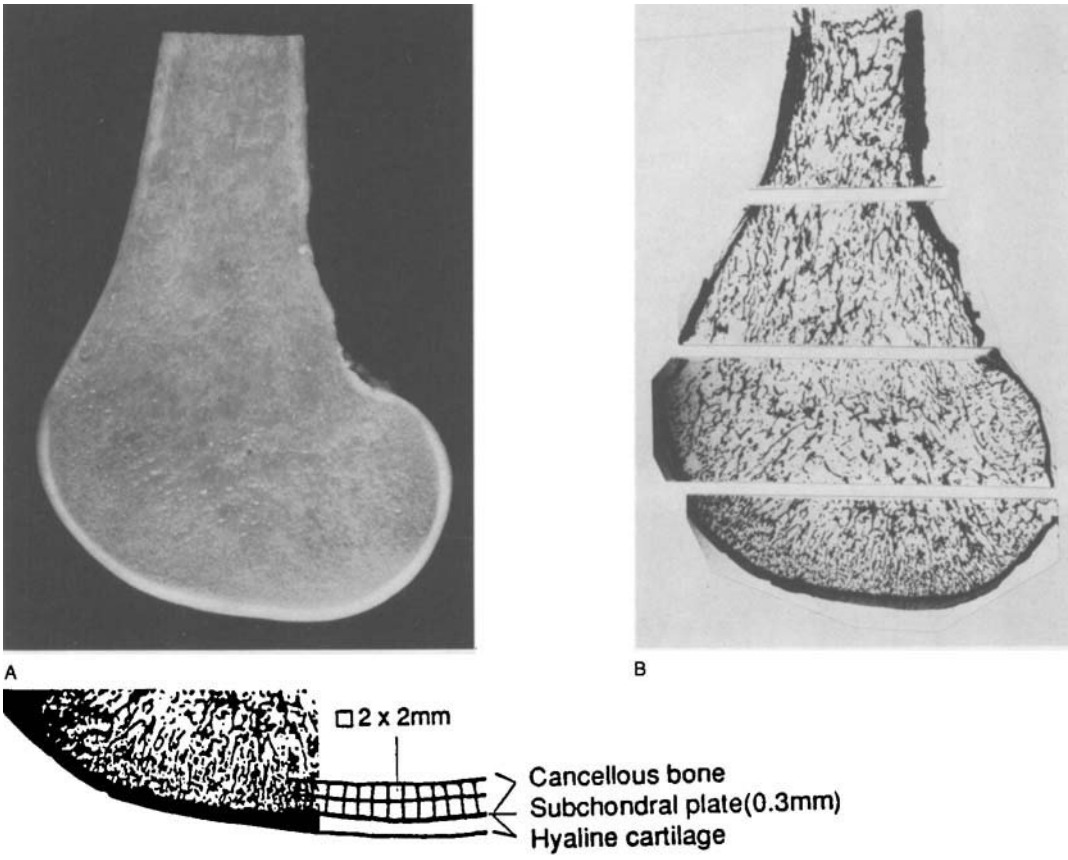

Figure 1.6. Normal joint structures.

A. Sagittal section through the lateral condyle of a 32-year-old man.

B. Corresponding histological section for the measurement of the relative bone density of the subchondral cancellous bone (2 zones, see graphic). Staining: Kossa.

C. Graphic.

A striking feature of the gradient-echo images was the difference in the apparent thickness of the articular cartilage before and after intraarticular administration of the contrast medium.

In addition, the contrast medium made possible an accurate assessment of the synovial surface, the cruciate ligaments, and of the menisci and their attachments.

MR-arthrography cannot solve the problem of distinguishing between hyaline articular cartilage and subchondral bone. This is because of the structure of the bone adjacent to the cartilage, the "smoothing programme" used to construct the image and the different radii of curvature of the joint surfaces.

The signal behaviour of the subchondral zone is determined by the bone-marrow, which contributes about 99% to the signal, and by the bone contributing only a minimal signal (1%).

In order to study the imaging of the junction of the hyaline cartilage, subchondral plate and subjacent cancellous bone in more detail, the relative densities were determined.

Method

The measurements were performed on the cadaver knee-joint of a 32-year-old man. After MRI-visualization of the knee-joint sagittal cuts were made through the lateral and medial femoral condyles. After an image had been produced without contrast medium (Figure 1.6), a slice of cartilage and bone 0.5-cm thick was taken for histologic workup, and the

Table 1.9. Average relative volume density (vVol%) of the cancellous bone and osteoid lying directly below the cartilage in the condyle (grid area 2 x 2 mm)

Part	Zone	Medial		Median		Lateral	
Anterior	1	21	*8.9*	28	*4.0*	19	*5.4*
	2	23	*7.2*			16	*4.0*
Middle	1	35	*9.9*	30	*7.2*	30	*5.6*
	2	28	*7.2*	31	*9.8*	22	*3.4*
Posterior	1	20	*6.1*			15	*4.4*
	2	16	*4.4*			13	*2.4*

histologic sections (Kossa staining) were then fitted together again to form a complete picture. The morphometric measurement of the bone density was carried out on the histologic pictures by the method of Merz (grid size L36) from two zones immediately adjacent to the subchondral plate (grid area 2 x 2mm; Appendix 2).

The measurements were carried out with 50-fold magnification, using a Leitz-ASM image analysis system. The densities of the mineralised bone and the osteoid were calculated using the method described by Delling.

Results

The subchondral plate with an average bone density of 95–100% and a width of 0.2–0.6 mm (average 0.3 mm), is abruptly contiguous with a zone of low bone density (Figure 1.6). In the next zone there is either a further slight decrease in the bone density or it remains constant (Table 1.9). There is a corresponding increase in the proportion of fat marrow. The bone density is not dependent on the degree of curvature, however. Less curved joint surfaces do not have a lower bone density than highly curved surfaces.

The consequence is that the normal subchondral plate of 0.3 mm, with a bone density of 95–100%, is not separately visualized, since its width lies below the pixel size. However, this zone and the subchondral bone component contribute jointly to the signal intensity of a pixel (Figure 1.7). The boundary between the cartilage and the subchondral bone as shown in an MR-image therefore appears broader than the anatomical structure of the subchondral plate (Figure 1.8).

This effect is reinforced by the "smoothing programme" used to construct the image in the computer. The signal intensity of a pixel on an MR-image represents the signal received from one volume element (voxel). The volume of the voxel corresponds to

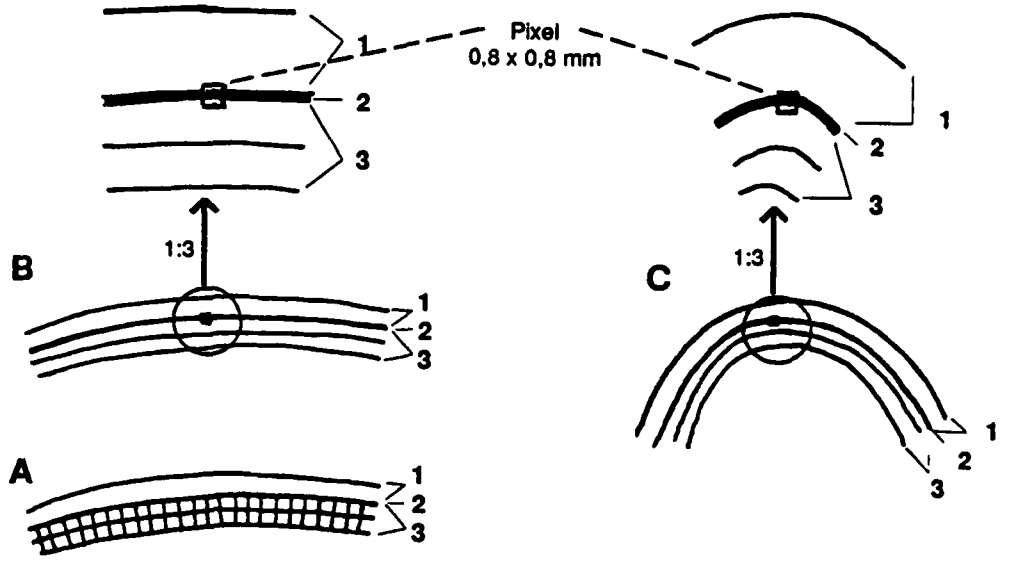

Figure 1.7. Normal joint structures. 1. Hyaline cartilage. 2. Subchondral plate (95–100 vVol%). 3. Cancellous bone (10–40 vVol%).

A. Width and bone density of the subchondral plate and also of the adjacent cancellous bone.

B. Edge-phenomenon, image made up of two zones of different relative volume density.

C. Image construction in a case of very curved section surfaces: apparent broadening of the subchondral, hypointense zone.

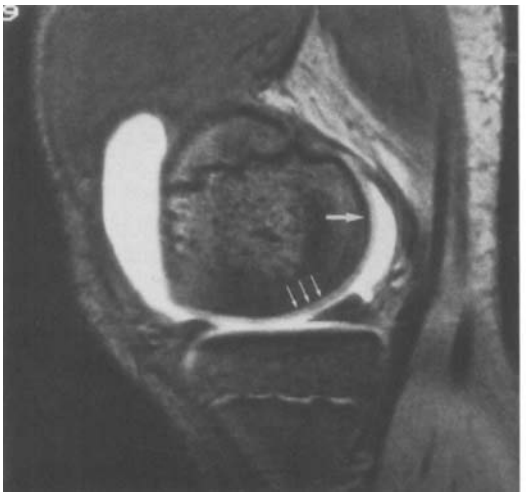

Figure 1.8. MR-arthrography (SE 700/15, sagittal plane, lateral condyle). Thin subchondral hypointense zone in the anterior, central, and parts of the posterior section of the condyle.
Broad subchondral hypointense zone from the center of the posterior part of the condyle.

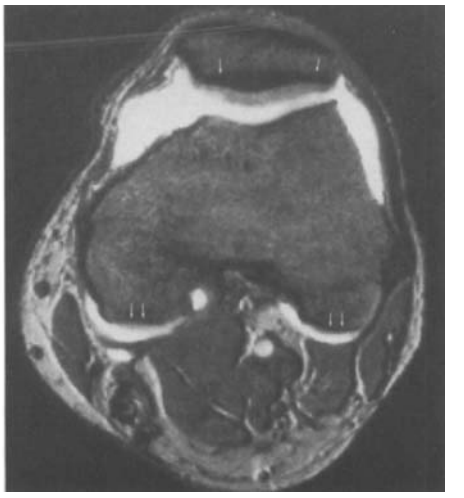

Figure 1.9. MR-arthrography (GE 30/10/30°, axial section). Subchondral hypointense zone, which is equally broad both at the femoral gliding surface of the patella, and at the medial and lateral condyle.

the area of a pixel multiplied by the thickness of slice used (T1: 1–5 mm slice thickness, GE-3D: 0.4–0.8 mm slice thickness). If a highly curved zone lies within a voxel (e.g. the posterior surface of the lateral condyle), then this will make a disproportionately large contribution to the emitted signal. It will therefore appear distinctly broader (Figure 1.7) even though the lowest relative bone density was measured specifically in the posterior part of the condyle.

Comments

The imaging of the structures adjacent to the cartilage is influenced to a considerable extent by the curvature in the slice plane, but this does not depend on the bone density of the subchondral zone. An ideal slice plane for measurement of the cartilage thickness will therefore take into account the differing curvatures of the joint surface and is informative only in those planes that show the least curvature (e.g., for the anterior and central parts of the condyles, sagittal-plane slices; for the patella and posterior part of the condyles, axial-plane slices (Figure 1.9). The normal width of the subchondral plate will not be visualized on these images, but will contribute to the hypointense zone between the articular cartilage and the subchondral bone. It is not until this has become broader in the context of advanced arthrosis and/or the zone of calcified cartilage has increased up to the pixel width, that it will be clearly distinguished by magnetic resonance imaging as of very low signal intensity. Since uncalcified cartilage shows a high signal intensity on GE-images, an increase in the calcification zone will be seen as a decrease in the breadth of the uncalcified cartilage. The zone of uncalcified cartilage cannot be differentiated from the calcified cartilage on T1-weighted images (see pages 33–34).

Assessment of the structural analysis of the hyaline cartilage by MR-arthrography

Fluid content of the hyaline articular cartilage

The assessment of the cartilage structure on T1-weighted and gradient-echo-sequence images is based on the water content, which influences the image. In healthy cartilage, a higher water content is found in the superficial layer than in the deeper layers. The opposite is true of the content of proteoglycans. Any disorders in the system, whether through an increased uptake of fluid (edema) or fluid loss (arthrosis) must therefore be reflected in altered signals. Yulish et al. [80] and Spritzer et al. [71] interpret hyperintense areas as focal swelling or a focal increase in the thickness of the cartilage. König et al. [44] and Cruess [14] also have reported local inhomogeneities. Cruess [14] considers that their clinical relevance is not yet clear, whereas König et al. [44] are prepared to draw conclusions about the condition of the hyaline cartilage from them—e.g., about the healing of grafts of cartilage and bone. In order to identify edematous areas of cartilage, these authors evaluated measurement areas of 1–2 mm^2 and gave their relative signal intensity.

Tyrell et al. [74] criticized the rigid view that the sole source of the image is the regional water content, pointing out that even when the water content remains constant, changes in the image may be induced within the articular cartilage by structural changes in the collagen.

Trace elements

Trace elements might also be able to influence the analysis of the cartilage structure. Of all the trace elements analysed in the cartilage, the iron content was of particular interest. Most of the iron is found in erythrocytes, bone marrow, reticuloendothelial system, muscle (myoglobin) and plasma. In man, the total iron content amounts to over 1 mmol/kg (35–50 mg/kg). This is distributed as follows: haemoglobin 62%, myoglobin 8%, enzymes containing iron 4%, ferritin 18%, and hemosiderin 8% [17].

The values found in the analysis of trace elements fluctuate from 10–125 ppm = 0.1–1.25 mg/kg. The plasma transferrin content is 4 mg/kg.

From investigations in hemophiliacs [37] it is known that hemosiderin is stored mostly in hyaline cartilage cells, and it has been demonstrated also in cartilage showing arthritic changes [12, 59]. In a study of rabbit-joint chondrocytes, Kirkpatrick et al. [42] were able to demonstrate that divalent and trivalent iron and hemoglobin are taken up into chondrocytes.

Aspiration in arthritic patients also showed an increased proportion of erythrocytes, as compared with normal plasma [64]. This suggests microhemorrhages from recent bone trauma or injuries of the capillaries of the granulation tissue (a manifestation of attempted repair), or alternatively the possibility of injury to the synovial membrane by osteophytes [57]. The stratum synoviale, a spongy, loose layer of cells which also contains newly formed blood vessels, is very vulnerable [19].

Newly formed synovial mast cells (synovial lining cells) also show an increased capacity to store haemosiderin [66]. The uptake of haemosiderin into the stratum synoviale and the stratum fibrosum, with fibrovascular proliferation and thickening of the capillaries, has also been described [53]. Our investigations have also found measurable amounts of iron particles (Table 1.10).

The question of whether the iron particles can induce a change in the signal intensity is of decisive im-

Table 1.10. Determination of iron element using an inductively coupled plasma-quadrupole mass spectrometer (ICP/MS) in articular cartilage and synovial membrane (ppm dry weight). Same case material as in Table 1.8

Case	Age	Sex	Medial femur		Lateral femur		Synovial membrane
			Zone 2	Zone 3	Zone 2	Zone 3	
1	67	f	20	69	50	140	230
2	83	m	< 10	50	< 10	15	190
3	57	m	40	< 10	250	< 10	1100
4	73	f	< 10	10	< 10	40	–
5	80	f	40	< 10	< 10	< 10	120
6	81	f	20	20	20	< 10	220
7	67	f	< 10	< 10	< 10	< 10	140
8	83	m	20	40	40	20	50
9	56	f	23	22	< 10	22	–
10	73	m	60	20	30	< 10	50

Table 1.11. Electron configuration of the first group of the transition elements (3d-ions) with spin quantum number and the magnetic moment observed

Ion	A	B					C	D
Ti^{3+}, V^{4+}	$3d^1$	↑					1/2	1.7–1.8
V^{3+}	$3d^2$	↑	↑				2/2	2.6–2.8
Cr^{3+}, V^{2+}	$3d^3$	↑	↑	↑			3/2	3.8
Mn^{3+}, Cr^{2+}	$3d^4$	↑	↑	↑	↑		4/2	4.9
Fe^{3+}, Mn^{2+}	$3d^5$	↑	↑	↑	↑	↑	5/2	5.9
Fe^{2+}, Co^{3+}	$3d^6$	↑↓	↑	↑	↑	↑	4/2	5.1–5.5
Co^{2+}	$3d^7$	↑↓	↑↓	↑	↑	↑	3/2	4.1–5.2
Ni^{2+}, Cu^{3+}	$3d^8$	↑↓	↑↓	↑↓	↑	↑	2/2	2.8–4.0
Cu^{2+}	$3d^9$	↑↓	↑↓	↑↓	↑↓	↑	1/2	1.7–2.2
Cu^{1+}	$3d^{10}$	↑↓	↑↓	↑↓	↑↓	↑↓	0	0

A Configuration
B Electron distribution
C Spin quantum number
D Magnetic Moment U_{eff} (Bohr Magnetrons)

Kittel C. Introduction to solid state physics. J. Wiley & Sons, New York, London, Sidney, 1968

Table 1.12. Electron configuration of the lanthanides group (trivalent 4f-ions) with spin quantum number and magnetic moment observed

Ion	A	B							C	D
Ce^{3+}	$4f^1$	↑							1/2	2.4
Pr^{3+}	$4f^2$	↑	↑						2/2	3.5
Nd^{3+}	$4f^3$	↑	↑	↑					3/2	3.5
Pm^{3+}	$4f^4$	↑	↑	↑	↑				4/2	–
Sm^{3+}	$4f^5$	↑	↑	↑	↑	↑			5/2	1.5
Eu^{3+}	$4f^6$	↑	↑	↑	↑	↑	↑		6/2	3.4
Gd^{3+}	$4f^7$	↑	↑	↑	↑	↑	↑	↑	7/2	8.0
Tb^{3+}	$4f^8$	↑↓	↑	↑	↑	↑	↑	↑		9.5
Dy^{3+}	$4f^9$	↑↓	↑↓	↑	↑	↑	↑	↑		10.6
Ho^{3+}	$4f^{10}$	↑↓	↑↓	↑↓	↑	↑	↑	↑		10.4
Er^{3+}	$4f^{11}$	↑↓	↑↓	↑↓	↑↓	↑	↑	↑		9.5
Tm^{3+}	$4f^{12}$	↑↓	↑↓	↑↓	↑↓	↑↓	↑	↑		7.3
Yb^{3+}	$4f^{13}$	↑↓	↑↓	↑↓	↑↓	↑↓	↑↓	↑		4.5

A, B, C, D As in Table 1.11.

Kittel C. Introduction to solid state physics. J. Wiley & Sons, New York, London, Sidney, 1968

portance for the imaging. Iron is present almost exclusively in Fe^{2+}- or Fe^{3+}-form, and, together with Cr^{3+}, Mg^{2+}, Mn^{3+}, Ni^{2+}, Cu^{2+} is classified in the group of the transition elements. The iron group has 18 electrons in closed shells and 1–9 electrons in the 3D-shell. The asymmetry and arrangement of the shell electrons result in a permanent paramagnetic moment. For individual electrons, this ranges from Cu^{+} 0 to gadolinium^{3+} 8 [26] (Tables 1.11 and 1.12).

If one now compares a 1 mmol/kg solution of iron (35–50 mg/kg) with the 2 mmol solution of Gd-DTPA used by us, this shows that there is a 4-times-greater magnetic moment with Gd^{3+}, or, in other words, values of 35–50 mg/kg iron would have the same influence on the enhancement as a 0.5 mmolar solution of Gd-DTPA. It therefore seems likely that the signal intensity of the hyaline cartilage can indeed be influenced by stored iron.

Comparison between measurements of the articular cartilage by MR-arthrography and histological section

The quality and information value of an imaging procedure which claims to assess the articular cartilage can be verified only by correlation with the histology. Accurate measurements of the thickness of the articular cartilage and of the size and area of cartilage fragments and defects are a basic prerequisite for this.

Measurements in the cadaver

The agreement between the subjective determination of surface marking points made by two experienced radiologists was tested. This was done in a comparison between MRI and MR-arthrography and also in a comparison of the cartilage thickness as measured on histological and cadaver preparations versus the MR studies.

Materials and methods

After imaging of the medial and lateral condyles of a knee-joint, with and without contrast medium (40 mL gadolinium-DTPA), with a spin-echo sequence T1 = 70°/15 and the gradient-echo sequences FLASH 3D and FISP 3D in the sagittal plane, the MRI-images were developed on a 1:1 scale. Slices ca. 10 mm thick were cut through the medial and lateral condyles, covering the whole area in the sagittal plane corresponding to the MR-image.

Black and white contact prints were produced photographically on a 1:1 scale from this fresh material. This was followed by fixation and the production of thin-slice preparations of the nondecalcified tissue (4 mm). These sections were stained, either by the modified silver staining method of Kossa (mineralised bone and cartilage appear black) or with toluidine-blue-O (calcified tissue appears unstained or pale blue, white cells, soft tissue and cartilaginous matrix stain in various shades of blue).

In this way it was possible to correlate the histological sections with the MRI-images, similarly reproduced in original size, as follows:

Colour copies of the histological sections were produced on a 1:1 scale on a transparent sheet by means of a laser copier. These copies were placed over the corresponding MR-images in such a way that 3 sectors of cartilage of identical curvature and the same location in the histological and MR-images coincided in each case (Figure 1.10).

To ensure the greatest possible accuracy, all of the marking work was carried out under a Zeiss stereomicroscope and with the use of a Schott light source KL 1500 in a bright field with x 1.5 magnification, and the reference marking distance, 2 cm in length, was drawn on the opaline glass.

At least 3 identical points on each of the three MR-images of the lateral or medial condyle in each case were marked by crosses (+) in such a way that they could be made to coincide. Then, using the technique described above, the marked points on the histological and MR-images, which defined 3 cartilage sectors per condyle in each case, were transferred on to the other MRI-images (Figure 1.11). The histological sections and MR-images marked up in this way were photographed on a 1:2.2 scale (Leica camera, Kodak

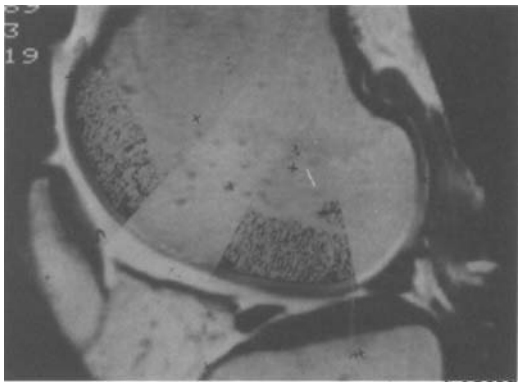

Figure 1.10. MR-arthrography (SE 700/15, GE 30/10/30°, FISP-3D, sagittal plane, lateral condyle). Montage of two copies (1:1) of two sectors from corresponding histological sections. Staining: Kossa.

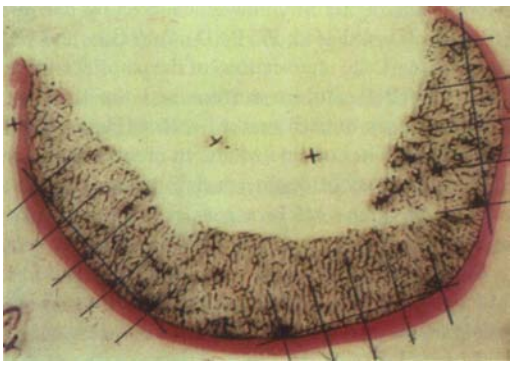

Figure 1.11. Macrograph of the large scale histologic section with a drawn grid system. Staining: Kossa.

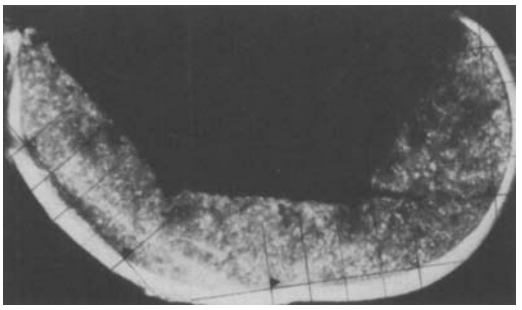

Figure 1.12. Sagittal section through the lateral condyle of a 29-year-old man. The grid system used for the assessment of the surface-cartilage thickness is added for the anterior, central and posterior part of the condyle.

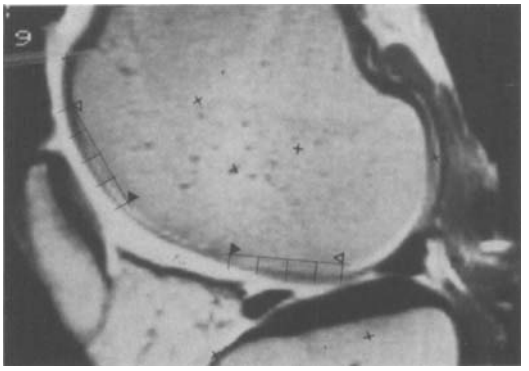

Figure 1.13. MRI, SE 700/15 (A), MR-Arthrography, SE 700/15 (B). The determination of the surface- and cartilage-thickness (A+B) drawn in by the assessor.

Ektachrome EPY 50, Ilford Pan F) and prints (13 x 18 cm) were made. Similar enlargements were also produced from the contact-prints of the fresh preparations of the medial and lateral condyles (Figure 1.12.). The marking of the sectors of cartilage to be measured was then transferred on to these black and white prints. In this way prints were finally obtained (13 x 18 cm), of the histology, the fresh preparation and the MR image on the same magnification scale of 1:2.6.

The cartilage/bone-boundary in the region of each marked sector represented approximately an arc of a circle, through which a chord 2 cm long was drawn. Straight lines were drawn at 5-mm intervals at right-angles to this chord so that the marked sector of cartilage was covered by a grid.

The surface and thickness of the cartilage were assessed as follows:

Two assessors worked independently of each other (A, B). Each received a complete set of the black and white prints of the MR images covered by the grid (FLASH 3D –Gd/+Gd; FISP 3D –Gd/+Gd), and was asked to mark the intersections of the parallel straight lines with the cartilage surface and the cartilage/bone-boundary in each marked sector (Figure 1.13). So as to be better orientated and in order to compensate for any loss of quality during the photographic processing of the MRI-images, each observer was also supplied with the original MRI-images.

The measurement of the 13 x 18 cm copies of the MR images marked up by the assessors, of the colour prints of the histological sections, and of the black and white prints of the fresh specimens was carried out using a semi-automatic image analysis system (IBAS KONTRON) with graphic tablet in the distance mode graduated in true size (mm) after the correct scale had been fed in by means of two-point transformation. A reference scale of 2 mm was always photographed as well.

The distance between the chord and the cartilage surface was used to assess the cartilage surface in each case. The cartilage thickness could be determined mathematically through subtraction of the distances between the cartilage/bone-boundary and the chord from the distances between the cartilage surface of the chord on each of the corresponding lines and could be analysed statistically (paired *t*-test [13]).

Results

The data show that for both assessors, regardless of the sequence technique used, the cartilage surface measurement points could be determined subjectively at all marking sites when gadolinium-DTPA had been used. But without contrast medium the surface could be determined subjectively in 75% (observer A = 70%, observer B = 80%) (Table 1.13). If, again regardless of the sequence technique used, one analyses the number of surface marking points determined by the two observers within a range of fluctuation of 0.3 mm (Table 1.14), then agreement was found in 39% of cases without intraarticular contrast medium and in 73% with contrast medium. The greatest number of measurement points that agreed was obtained with T1 plus Gd, and the smallest number with T1 without Gd.

The difference for all evaluable measurement points between the two assessors amounted to –0.18 ± 0.1 (FLASH 3D) and –0.13 ± 0.07 (FISP 3D) with-

Table 1.13. Number of surface measurement points (N 30) which could not be determined subjectively

	MRI		MR-arthrography	
Observer	A	B	A	B
T1	80	3	0	0
FISP 3D	9	8	0	0
FLASH 3D	10	8	0	0

Table 1.14. Number of marking points (N 30) assessed by both observers as showing agreement within a range of fluctuation of 0.3 mm

	MRI	MR-arthrography
T1	11	26
FISP 3D	12	21
FLASH 3D	12	19

Table 1.15. Comparison of subjective surface determinations by two observers. Mean, *SD*

	MRI	MR-arthrography
T1	-0.15 *0.1*	-0.02 *0.04*
FISP 3D	-0.13 *0.07*	-0.16 *0.04**
FLASH 3D	-0.18 *0.11*	+0.12 *0.11*

* $p = 0.05$

Table 1.16. Difference in thickness of cartilage between the plain image and MRI / MR arthrography (mm)

	Plain image vs. MRI	Plain image vs. MR-arthrography
T1	-0.41*	-0.35*
FISP 3D	+0.09	-0.24*
FLASH 3D	-0.08	-0.18*

* $p = 0.05$

out contrast medium. With contrast medium, the difference was 0.02 ± 0.04 (T1) and 0.2 ± 0.11(FLASH 3D) (Table 1.15).

In comparison with the thickness of cartilage measured on the unprocessed specimen, the subjective determination of the thickness without the use of intraarticular contrast medium (75% of the measurement points being evaluable), resulted in a overestimation (p = 0.05) for T1-weighted images, whereas the GE-images did not show any difference. In MR-arthrography, a difference from the directly measured thickness was obtained with any of the sequence techniques (Table 1.16).

The difference in measured thickness of cartilage between the unprocessed specimen and the large-scale histological sections (Kossa staining, toluidine blue) averaged about 10%, a constantly smaller thickness being measured in the histological sections.

Comments

A constant and reproducible assessment of the cartilage surface, which is independent of the investigators and shows agreement between them, is possible through MR-arthrography. This applies to all parts of the knee-joint and all sequence techniques. An adequate assessment of the surface is possible in 74.5% without contrast medium, but with less good agreement (50%) between the observers than with MR-arthrography. Since the determination of the surface is a necessary prerequisite for measurement of the cartilage thickness, MR-arthrography represents the method of choice. There may be various reasons for the significant underestimation of the cartilage thickness in MR-arthrography by comparison with the unprocessed specimen. It might be due to fluid absorption, leading to swelling of the cartilage (absence of loading-pressure, breakdown of the collagen). This assumption is supported by the fact that similar phenomena occur when cadaver cartilage is in fairly prolonged contact with gadolinium-DTPA [62]. One might also be dealing with an over-irradiation phenomenon here, due to a marked difference in signal intensity between the articular cartilage and gadolinium-DTPA. This difference is minimal however, and is less than the width of one pixel.

The investigation demonstrates two important points:

– The determination of the cartilage surface is independent of the investigators with the use of MR-arthrography.

– Measurement of the cartilage thickness on cadaver cartilage is associated with some inherent uncertainty factors (swelling, altered behaviour of contrast medium compared with articular cartilage) and the findings should therefore not be extrapolated to the situation in vivo.

It should also be noted that the fixation of a histologic section causes the cartilage preparation to shrink by about 10%. A correction factor must there-

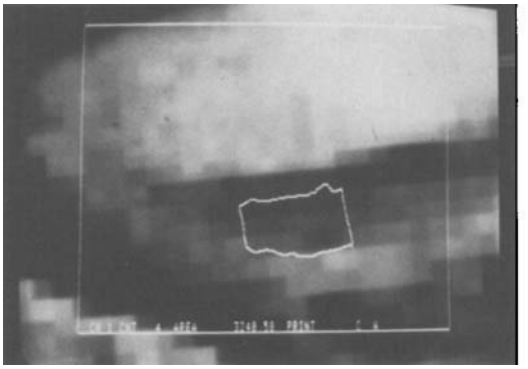

Figure 1.14. T1-weighted image (section) enlarged and projected on to the monitor. The cartilage area to be measured is outlined with the cursor.

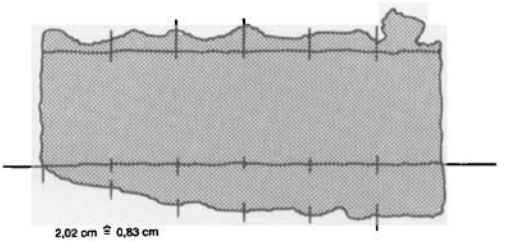

Figure 1.15. Graphic presentation after the cartilage area and thickness to be measured have been marked (area-presentation in accordance with the histologic section).

fore always be included in the calculations when considering cartilage thickness measured on histological sections. This applies both in vivo and in vitro.

Results after administration of the contrast medium in vivo

In 20 patients with severe gonarthrosis, MR-arthrography was performed with Gd-DTPA prior to an operation on the knee. The pieces of cartilage and bone, taken in accordance with accepted surgical technique, were divided in correspondence with the MR-plane of section and prepared for histology (hematoxilin-eosin staining). Twenty histological sections from 11 patients, whose MR images and histological sections could be unequivocally correlated, were evaluated.

Measurement of the histological sections

The histological preparations were projected on to a colour monitor via a stereo-microscope (Zeiss SV 8) connected to a VIDEO-camera (Sony, Trinicon). The measurements were performed with a semi-automatic IBAS KONTRON with graphic tablet in the TV-mode. At a point which was reproducible in the MR image a straight line was drawn parallel to the subchondral zone. Through the use of a square grid (width: 1 mm) an area 5 mm in length and vertical to the straight line was defined, outlined by the cursor, and in this way the size of the cartilage area was determined (in relative figures due to the magnification factor of the microscope and camera; Figure 1.14). The outlined area was printed out graphically by the attached thermo-printer.

On the basis of the graphics, the cartilage thickness was determined at 7 points (at a distance of 0.83 mm in each case) by means of semi-automatic image analysis using two methods (Figure 1.15).

Method A

Measurement of the cartilage thickness in millimeters (absolute figures) was carried out by means of 2-point transformation after the correct scale had been fed in. The reference parameter was a stage-micrometer of 200 μm, which was also printed out graphically after magnification.

Method B

Determination of the cartilage thickness as a relative figure was carried out in the distance mode with division through the magnification resulting from the microscope and camera objective and reduced graphic printout with a total magnification factor of 24.24.

Measurement of the MR-images

The relevant reference parameters (thickness, area) for the SE- and GE-images were determined as described in the above procedure. The corresponding reducing factor of the MR-images was taken into account.

Statistics

The area measurements and cartilage thickness determinations were carried out separately by groups (histology, T1, FLASH) and also in correlation with one another. The mean value and standard deviation were calculated and also the correlation between the histology and SE-sequences and between the histology and GE-sequences using the Pearson coefficient of correlation on the assumption of a normal distribution. In order to be able to assess the closeness of the relationship between the individual parameters, the differences between the area measurements and the cartilage thickness measurements were tested with the *t*-test for their significance at the 5%-level [13]. The analysis was carried out for both methods of calculation.

Results

The area calculations showed a good correlation between the histology and T1-images but not between the histology and GE-sequences (Table 1.17, Figure 1.16).

There was agreement between the areas for the histology and the T1-images in 83% and for the histology and GE-images in 42%. The *t*-test did not show any difference between the histology and the T1-images, but it did between the histology and the GE-images.

The analysis of the cartilage thickness measurements calculated by two methods (Table 1.18) showed a correlation between the histology and T1-images but not between the histology and GE-sequences (Figures 1.17 and 1.18), with 65% definite agreement between the histology and T1 images with both measurement methods. The corresponding figures for the GE-images were 11% and 14%, respectively. The calculation of the mean values for all the distance data showed that the cartilage thickness was constantly slightly overestimated on the T1-images, whereas the cartilage thickness was distinctly underestimated on the GE-images. The significances were chiefly due to the large number of random samples and the fact that the mean values of T1 were higher—although only slightly—than those for the histology, whereas the FLASH-mean values were lower than those for the histology.

Comments

The use of a contrast medium as a medium for the imaging of boundary surfaces in MR-tomography has made it possible to distinguish more accurately between the cartilage surface area and the joint cavity. As a result the surface areas and thickness of the cartilage can be measured. Analysis of the measurement data showed that there was greater agreement between the image and the histology in T1-weighted images than with the gradient echo sequences, so that the former are also more suitable for the in vivo assessment of cartilage surface- or thickness-measurements. The overestimation of the area and thickness by about 0.1 mm in the T1-weighted images is clearly negligible and is probably due to the pixel size of 0.8 × 0.8 × 1 to 2 mm and to the difficulty in measuring a curved surface area despite the small section measured.

Besides the accurate determination of the cartilage surface, for the assessment of the cartilage thickness by means of the MR-image it is of the greatest importance that the hyaline cartilage should be accurately demarcated from the subchondral bone.

This is not possible to the same extent with T1-weighted and gradient-echo-images however. The thickness of the cartilage visualized in the T1-image is minimally greater than the actual cartilage thickness. The overestimation of the cartilage thickness might also be a signal effect—induced through a so-called "edge-phenomenon".

In GE-images (FLASH 2D) an inhomogenous picture of the cartilage is seen, with an underestimation of the cartilage thickness and an "overestimation of the covering bone plate".

Table 1.17. Area data of T1-, GE-images, and areas identical to these on the histological sections (mm²). Mean, *SD*

Histology (n 20)	**11.9**	***2.71***
T1 (n 16)	**12.4**	***2.98***
FLASH (n 12)	**9.9**	***1.28***

Table 1.18. Cartilage thickness measured on the T1- and GE-images and also on the corresponding pictures of the histological sections (mm). Mean, *SD*

	Method 1		**Method 2**	
Histology (n 140)	**2.23**	***0.56***	**2.23**	***0.56***
T1 (n 112)	**2.36**	***0.61***	**2.35**	***0.61***
FLASH (n 91)	**1.98**	***0.41***	**1.97**	***0.43***

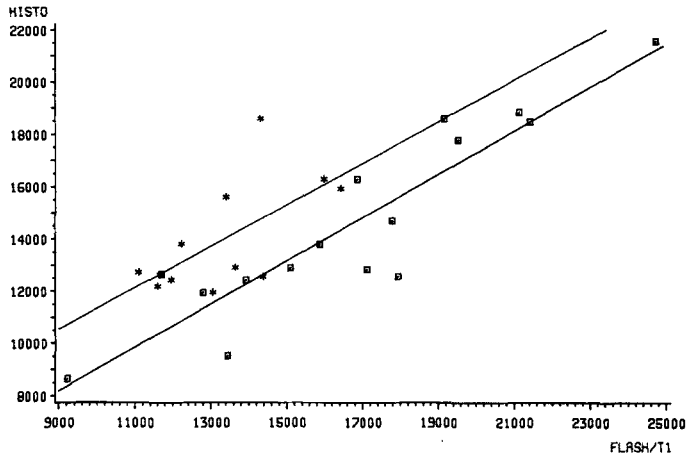

Figure 1.16. Correlation between the area-calculation by histology compared with T1 and FLASH-2D. * Flash and □ T1.

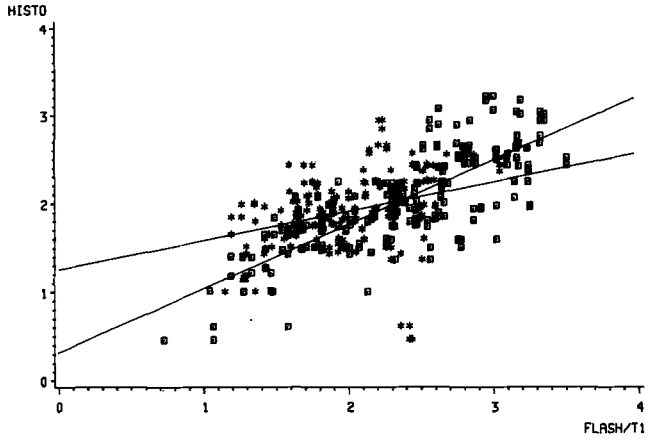

Figure 1.17. Correlation between the calculation of the cartilage thickness by histology compared with T1 and FLASH-2D, Method 1. * Flash and □ T1.

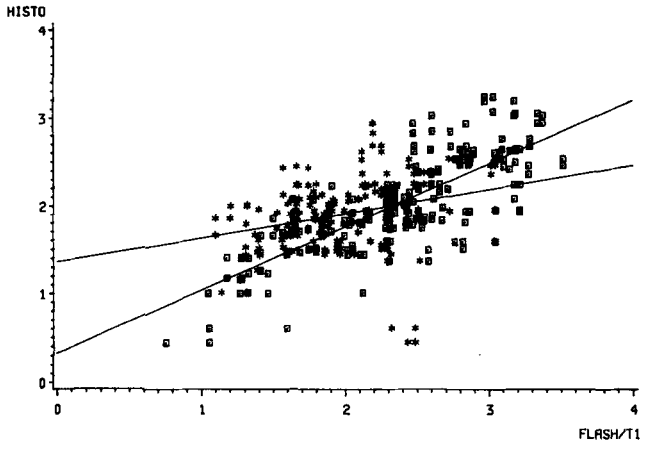

Figure 1.18. Correlation between the calculation of the cartilage thickness by histology compared with T1 and FLASH-2D, Method 2. * Flash and □ T1.

Since the subchondral plate is only one tenth of a millimeter wide, this layer most probably corresponds to the layer of calcified cartilage. In cases of arthrosis this layer becomes broader and a doubling or tripling of the tidemark occasionally occurs [25] so that the cartilage thickness measured therefore corresponds to the thickness of the layer of uncalcified cartilage.

It is not possible to differentiate between calcified and uncalcified layers of cartilage in the T1-weighted image. A visual distinction between the covering bone plate and the adjacent subchondral bone and the hyaline cartilage is possible in the T1-weighted image. In a GE-sequence such a distinction can be made between calcified and uncalcified layers of cartilage.

Conclusions

1. Gd-DTPA is a contrast medium which is suitable for intraarticular use in MR-arthrography.

2. 30–40 mL of a 2 mmolar solution is recommended as the ideal concentration.

3. In this concentration Gd-DTPA brings about optimal contrast of the internal joint structures without inducing any reaction of the synovial membrane.

4. The molecular structure of Gd-DTPA does not prevent it from being taken up into the intercellular fluid space. This process is transitory and reversible. It has been demonstrated that no increased concentration of gadolinium could be measured in vital human cartilage after 17 hours.

5. The intraarticular administration of the contrast medium makes possible accurate and constantly reproducible imaging of all joint structures and is superior to the examination carried out without the use of contrast medium. This particularly applies to the imaging of the surface of the articular cartilage.

II. Technique

The clinical section deals with the results of investigations obtained on 73 patients (31 female, 42 male). The ages of these patients ranged from 13 to 83 years (Table 2). The indications for the MRI-examination with and without contrase medium were chondral or osteochondral defects, degenerative changes of the knee-joint or other forms of damage to the internal structure of the knee, such as lesions of the menisci and synovitis.

Table 2. Age distribution of the patients investigated by MR-arthrography

Age	10–	20–	30–	40–	50–	60–	70–	>80
n	10	14	20	4	7	7	7	4

MR-arthrography investigation technique

The technique required to introduce the Gd-DTPA into the knee-joint differs only slightly from that currently used for intraarticular injection [75, 54].

For the administration of Gd-DTPA the knee joint is placed in a slightly bent, recumbent position for antero-lateral access or in a hanging position for intrapatellar access. In order to be able to fill the internal cavity of the knee with a small amount of contrast medium dissolved in physiological NaCl-solution, compression is applied to the soft tissues 15–20 cm above the joint cavity with an elastic bandage (Figure 2.1). The injection itself is carried out under sterile conditions. The amount of dissolved and injected contrast medium is 30–40 mL. After the injection, intensive active and passive movements of the knee joint are carried out several times in order to achieve uniform distribution in the joint. This is followed by the magnetic resonance imaging examination.

This was performed on all patients using a 1.5 Tesla machine (Magnetom 63, Siemens company, Erlangen, FRG). T1-weighted images were always produced, T2-weighted images in only a few cases. The use of gradient-echo sequences was initially carried out with FLASH 2D (n = 20 patients) and afterwards with the FISP 3D-gradient-echo technique (n = 53 patients). A surface coil (knee resonator) 20 cm in diameter was used for all the examinations. The examination time for T1-sequences was 6 min, and for the 2D and 3D-gradient sequences 8 min.

Technical errors in carrying out the MR-arthrography

The injection of the contrast medium did not always result in the desired intraarticular administration. In 4 examinations the contrast medium was injected into the periarticular soft tissues or into a pre-formed hollow cavity, which resulted in no or inadequate visualization of the joint surface. More specifically the mistakes were attributable to inadequate technique (2

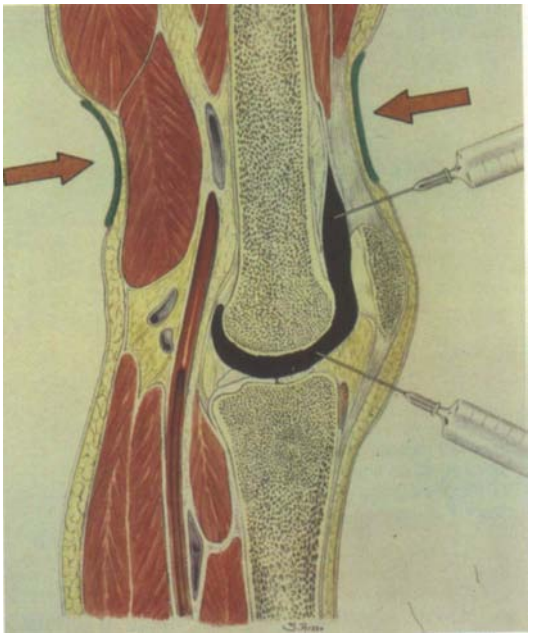

Figure 2.1. Illustration of the injection technique used, upper recess reduced in size through compression with an elastic bandage.

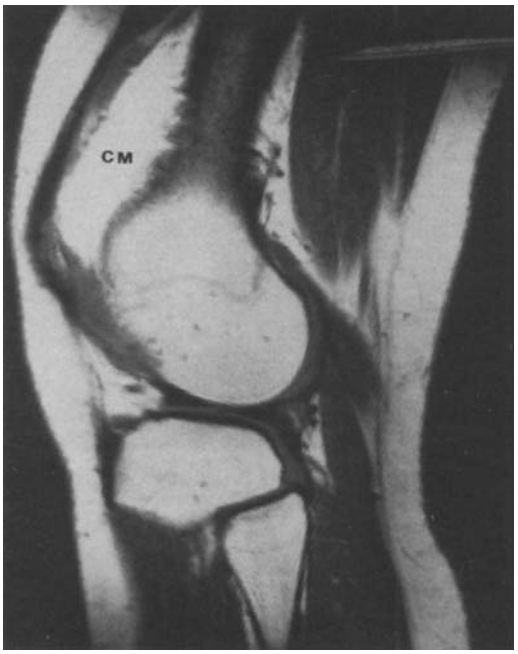

Figure 2.2. Sagittal plane, lateral condyle, SE 700/15. Administration of the contrast medium (CM) into parts of the quadriceps femoris muscle.

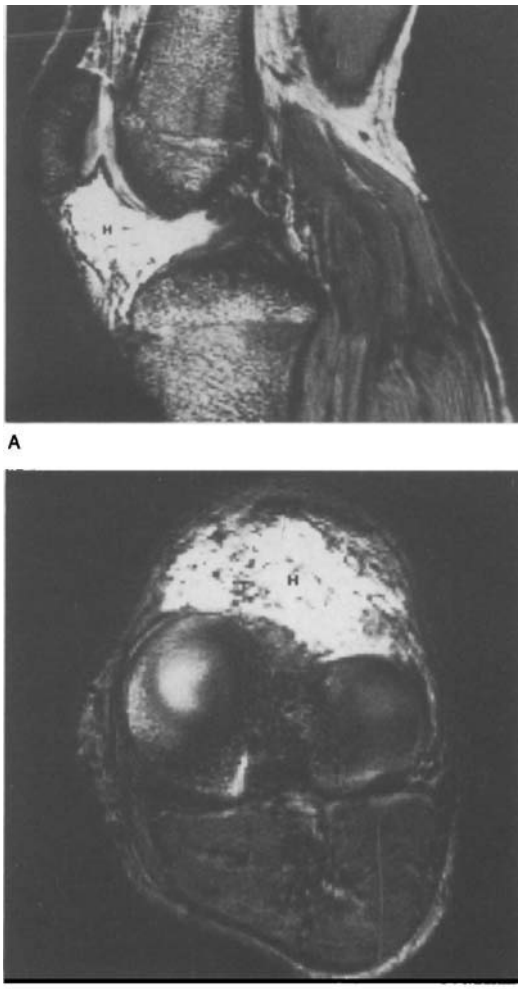

Figure 2.3. GE 30/10/30°.

A. Median sagittal plane. Administration of the contrast medium into the infrapatellar fatty body of Hoffa (H).

B. Axial plane.

cases), wrong choice of access route (1 case) and an existing pathologic internal knee structure (1 case). This corresponds to a failure rate of 8.1%.

Inadequate technique

1. Injection of contrast medium into the subcutaneous adipose tissue or parts of the quadriceps femoris muscle in the case of antero-lateral access (Figure 2.2).

In elderly people with marked obesity, it is not always easy to insert the injection needle into the upper recess. The subcutaneous adipose tissue readily permits wide distribution of the contrast medium after only slight pressure on the plunger, thus simulating intra-articular administration. If the injection is made into muscle tissue, greater pressure on the plunger is required, and the injection is also painful.

2. Injection of contrast medium into the infrapatellar fatty body of Hoffa in the case of infrapatellar access (Figure 2.3).

The use of too short a needle or the proliferative development of villi in the infrapatellar fatty body of Hoffa cause the contrast medium to be distributed in the adipose tissue. This results in a painful, but not long-lasting state of tension.

Wrong choice of access route

When marked synovitis is present, villi or septa may prevent uniform distribution of the contrast medium

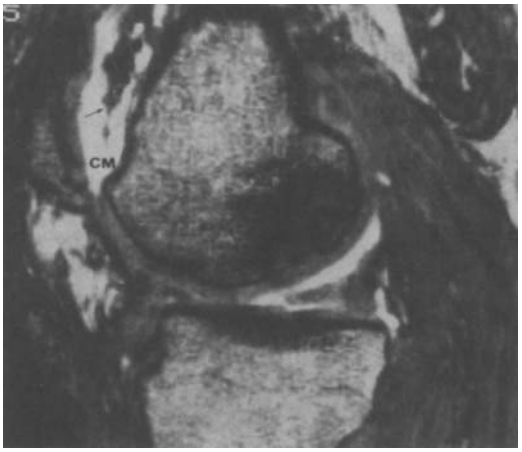

Figure 2.4. Sagittal plane, medial condyle, GE 30/10/30°. Technique with antero-lateral access. Contrast medium distribution (CM) impaired by marked synovitis (arrow).

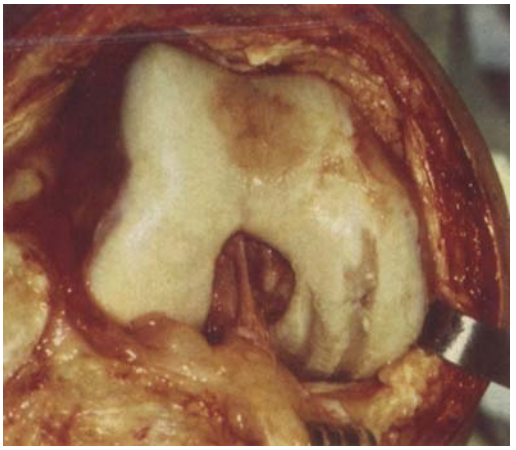

Figure 2.5. Operation picture. Broad cartilage defect in the weight-bearing zone of the medial condyle.

with the use of a antero-lateral access route, so that the articular cartilage is inadequately visualized (Figures 2.4 and 2.5).

In these cases, but also in severe arthrosis of the knee with bone deformities, it is advisable to choose an infrapatellar access route, since after filling of the intercondylar space, only a slight degree of movement can readily distribute the contrast medium sufficiently for visualization of the cartilage.

Pathologic internal knee-joint structures

Besides marked synovitis, the development of a closed, sacciform compartment of the upper recess is often found (Figures 2.6 and 2.7).

If the contrast medium is injected into this, pain due to tension is caused relatively late. This first happens when the bursa has been completely filled with contrast medium. A primary distinction between the internal knee cavity and the bursa is not possible.

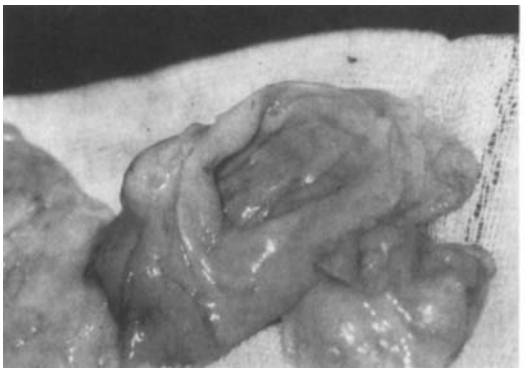

Figure 2.6. Joint capsule tissue with saccular evagination in arthrosis of the knee.

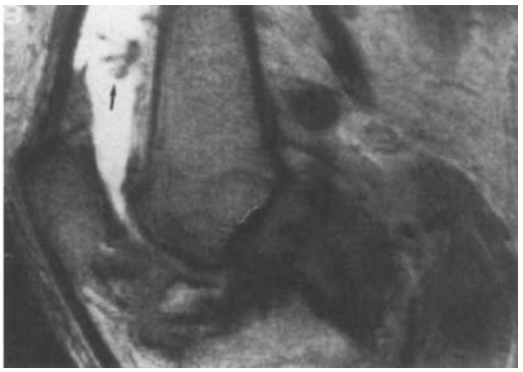

Figure 2.7. MR-arthrography (GE 30/10/30°, sagittal plane). Accumulation of contrast medium (CM) in a compartmentalized region of the joint capsule synovial villus (arrow).

Comments

Mistakes in MR-arthrography can be avoided through the use of the correct injection technique. If, however, changes of the upper recess are already present and have already been indicated by the clinical examination, it is advisable to carry out a T1-weighted scan prior to the MR-arthrography.

This makes it considerably easier to select the correct access route.

Conclusions

1. Contrast medium is administered into the knee-joint in the same way as with the customarily used injection techniques, but suprapatellar compression is additionally applied.

2. The inadvertent administration of Gd-DTPA into the musculature and the infrapatellar fatty body of Hoffa does not lead to any contrast medium-specific tissue reactions.

III. Clinical relevance

Comparison of pathological findings with and without contrast medium

MRI-findings in patients with gonarthrosis

This group consisted of 20 patients (6 men, 14 women) with an average age of 70 ± 9.3 (56–83) years. Preoperatively, 13 patients were using 2 underarm support crutches, 12 of these managing a walking distance of 100–500 m. Eight patients managed a walking distance of between 1000 and 1500 m. All of the patients were operated on with a knee endoprosthesis. The radiographs before the operation showed severe arthrosis.

The MRI-images were evaluated retrospectively (Tables 3.1 and 3.2.). The comparison of the findings obtained before and after the administration of the contrast medium underlines the value of MR-arthrography for the assessment of the hyaline cartilage and the synovial membranes. In the detail of the images it is possible to distinguish between bare bone, areas with remains of cartilage or a focal chondromalacia.

The comparison of the sequences used showed that for the assessment of the cartilage, the FLASH + Gd-images showed the best agreement with the plain image and the histology (Table 3.3).

The agreement between T1 and Gd compared with FLASH and Gd, fluctuated between 84% and 94% depending on the location.

MR-findings in patients with knee symptoms

This group of 53 patients (36 men, 17 women) had an average age of 33 ± 13 (13–72) years. None of the patients used a walking aid or showed any impairment of walking ability up to 3000 m. Radiographically, signs of minimal arthrosis were present in only 6 pa-

Table 3.1. Retrospective assessment of pathological cartilage changes with and without contrast medium

Case	Age	Sex	Medial condyle				Lateral condyle				Patella			
			T1	GE	T1-Gd	GE-Gd	T1	GE	T1-Gd	GE-Gd	T1	GE	T1-Gd	GE-Gd
K.G.	56	f	1	1	1	2	1	1	2	2	5	1	1	1
R.M.	73	f	4	4	4	4	2	2	2	2	1	2	2	2
S.B.	67	f	4	4	4	4	1	2	2	2	5	5	2	2
Z.T.	81	f	4	4	4	4	5	5	2	2	2	2	2	2
G.R.	58	f	4	4	4	4	1	1	1	2	2	2	2	2
F.B.	73	m	–	–	2	2	–	–	2	2	2	2	–	–
K.F.	82	m	–	–	2	2	–	–	4	4	2	2	–	–
M.M.	59	f	4	2	2	2	4	5	2	2	2	2	2	2
K.R.	64	f	4	4	4	3	1	1	1	1	2	2	2	2
H.E.	68	f	5	2	4	2	1	1	1	1	1	1	2	2
L.H.	62	f	4	4	4	4	4	4	3	3	4	4	3	3
M.J.	63	f	4	2	3	3	4	2	4	4	4	4	3	3
B.J.	83	f	4	5	3	3	4	4	4	4	4	4	4	4
C.B.	80	f	2	2	2	2	2	4	4	4	1	1	2	2
T.J.	57	m	5	2	2	2	5	2	3	4	5	5	1	1
G.M.	75	f	4	4	4	4	1	2	2	2	1	1	2	2
H.C.	59	f	1	2	1	2	1	1	1	1	1	1	1	1
W.E.	67	f	4	4	–	–	1	1	–	–	5	5	–	–
R.G.	82	m	4	4	4	4	2	2	2	2	2	2	2	2
T.A	79	f	2	2	2	2	5	2	2	2	1	1	1	2

1 normal
2 chondromalacia
3 bare bone with remains of cartilage
4 bare bone
5 not evaluable
– no data

Table 3.2. Retrospective assessment of pathological knee-joint changes with and without contrast medium

Case	Age	Sex	Meniscal lesion				Cruciate lig. lesion				Synovitis				Change in Hoffa-body			
			T1	GE	T1-Gd	GE-Gd	T1	GE	T1-Gd	GE-Gd	T1	GE	T1-Gd	GE-Gd	T1	GE	T1-Gd	GE-Gd
K.G.	56	f	5	5	5	5	2	1	1	0	2	1	1	1	0	0	0	0
R.M.	73	f	3,6	9,6	3,0	3,6	1	1	1	1	2	2	1	1	3	3	3	3
S.B.	67	f	2	2	2	2	2	2	0	0	3	3	1	1	1	1	1	1
Z.Th.	81	f	4,6	4,6	4,6	4,6	1,4	1,4	1	1	2	2	1	1	3	3	3	3
G.R.	58	f	2	2	2	2	0	0	0	0	1	1	1	1	3	3	3	3
F.J.	73	m	–	–	2	2	–	–	1	1	–	–	1	1	–	–	1	1
K.F.	82	m	–	–	4,6	4,6	–	–	1	1	–	–	1	1	–	–	2	2
M.M.	59	f	2,7	2,7	3,7	3,7	2	2	1	1	3	3	1	1	1	1	1	1
K.R.	64	f	2	2	2	2	2	0	2	0	0	1	1	1	1	1	1	1
H.E.	68	f	2	2	2	2	0	0	0	0	2	2	1	1	1	1	1	1
L.H.	62	f	3,8	3,8	3,8	3,8	1	1	1	1	2	2	1	1	1	1	1	1
M.J.	63	f	3,8	3,8	3,8	3,8	1	1	1	1	1	1	1	1	1	1	1	1
B.J.	83	f	2,8	3,8	3,7	3,7	1	1	1	1	2	2	2	2	1	1	1	1
C.B.	80	f	2,8	2,7	2,7	2,7	0	0	0	0	2	2	2	2	1	1	1	1
T.J.	57	m	2,7	2,7	2,7	2,7	2	1	1	0	2	2	1	1	2	2	2	2
G.M.	75	f	3,6	3,6	3,6	3,6	1	1	1	1	2	1	1	1	2	2	2	2
H.C.	59	f	1	1	1	1	0	0	0	0	0	0	0	0	0	0	0	0
W.E.	67	f	4,6	4,6	–	–	1	1	–	–	2	2	–	–	3	3	–	–
R.G.	82	m	3,6	3,6	3,6	3,6	2	2	2	1	0	2	0	0	1	1	1	1
T.A.	79	f	3,6	3,6	3,6	3,6	0	0	0	0	2	2	1	1	1	1	1	1

Meniscal lesions
0 normal
1 medial meniscal lesion
2 medial meniscal lesion + degenerative changes
3 medial residual meniscus
4 medial meniscus absent
5 lateral meniscal lesion
6 lateral meniscal lesion + degenerative changes
7 lateral residual meniscus
8 lateral meniscus absent
9 not evaluable

Cruciate ligament
0 normal
1 anterior cruciate ligament lesion
2 anterior cruciate ligament not evaluable
3 posterior cruciate ligament lesion
4 posterior cruciate ligament not evaluable

Synovitis
0 normal
1 synovitis
2 effusion
3 not evaluable

Hoffa
0 normal
1 medial hypotrophy
2 lateral hypotrophy
3 medial and lateral hypotrophy

Table 3.3. Comparison of the information value of different sequences with and without contrast medium on the basis of changes in the hyaline cartilage

	Assessment	T1 vs. Flash+Gd	T1 vs. T1+Gd	Flash vs. Flash+Gd	T1+Gd vs. Flash+Gd
Medial condyle	same	9	12	13	16
	different	8	5	4	3
Lateral condyle	same	7	8	10	17
	different	10	9	7	2
Patella	same	10	8	10	16
	different	7	9	7	1

tients. Forty-nine patients from this group actively practised some kind of sport up until the MRI-examination.

The evaluation (Appendix 3) showed that pathological changes of the cartilage represent the primary indication for MR-arthrography (Table 3.4) This is also true when a diagnosis can be made, even without contrast medium, since clinically relevant questions of detail (e.g., the stages of osteochondritis dissecans) can sometimes only be answered by MR-arthrography.

Table 3.4. Clinical use of MR-arthrography. Detection of pathological changes with and without contrast medium (N 53)

		Before injection		MR-arthrography	
	n	T1	GE	T1	GE
Chondromalacia	33	8	8	28	33
Osteochondritis	10	10	10	10	10
Loose joint body	5	4	4	5	5
Meniscal lesion	18	17	17	18	18
Synovitis	14	1	1	14	14
Plica syndrome	9	-	-	9	9
Lesion of the cruciate lig.	4	4	4	4	4
Bone changes	22	22	22	22	22

Table 3.5. Comparison between diagnostic clinical-, MR-arthrography-, and operation findings

Case	Age	Sex	Side	Diagnostic clinical	MR-arthrogr. findings	Operative findings
O.N.	20	f	l	1	3	3
K.W.	60	m	l	4, 8	2, 8	2, 8
I.R.	68	m	l	2, 8	2, 6, 8	2, 8
W.M.	27	f	r	2, 8, 9	2, 9, 8	2, 9, 8
B.G.	29	m	l	1, 8	–	–
St.I.	22	f	l	13	1, 8, 13	1, 8, 13
H.K.	34	m	l	1	1, 4	1, 4
K.C.	20	m	r	1, 10	3, 10	3, 10
G.H.	35	m	r	1	4	4
F.E.	47	f	r	1	1	1
L.F.	18	f	l	1	1	10
S.D.	35	m	r	12	12	12
S.S.	20	f	r	1, 8	8	8
G.F.	55	m	l	1, 4, 8	1, 4	1, 4
W.E.	37	f	l	1, 9	1, 2, 9	1, 2, 9
W.W.	35	m	r	1, 11	6, 7	–
U.G.	19	f	r	1, 12	1, 12	1, 12
T.A.	55	f	r	15	1, 2	1, 2, 8
F.S.	33	f	l	1, 13	1, 2, 8, 13	1, 2, 8, 13
E.G.	17	m	r	9	9	9
K.K.	35	m	r	1, 14	1, 10, 14	1, 10, 14
W.H.	37	m	l	4	4	4
H.K.	46	m	r	8, 9	4, 8, 9	8, 9
M.N.	27	m	l	2, 3	2, 3, 8	2, 3, 8
T.O.	26	m	r	12	12	12

1 Chondromalacia patellae
2 Chondromalacia medial condyle
3 Chondromalacia lateral condyle
4 Medial meniscal lesion
5 Lateral meniscal lesion
6 Medial intrameniscal degenerative changes
7 Lateral intrameniscal degenerative changes
8 Synovitis
9 Rupture of ant. cruciate ligament
10 Plica suprapatellaris
11 Patella-top syndrome
12 Osteochondritis dissecans
13 Loose joint body
14 Fracture of the patella
15 Chondromatosis

Table 3.6. Agreement between MR-arthrography- and operation-findings and also between diagnostic clinical- and operation-findings (percentages)

	MR-arthrography vs. Operation-findings	Diagnostic clinical- vs. Operation-findings
Sensitivitty	91.6	71.8
Specifity	99.1	92.6
Accuracy	98.5	95.8
False negative findings	1.8	4.7
False positive findings	4.3	39.1

Comments

The diagnostic clinical-, MR-arthrogaphy-, and operation-findings, obtained in that order, illustrated the problems of making a clinical diagnosis, and also the marked agreement with the findings obtained by arthroscopy or arthrotomy (Table 3.5).

MR-arthrography possesses great sensitivity and specificity with only a very small percentage of false-positive or false-negative findings (Table 3.6). This result is better than that for double-contrast arthrography and high-resolution-CT [68, 48, 16, 67, 24]. A comparison with the data given for the accuracy rates of MRI without contrast medium is difficult, because prospective figures are available only for specific regions (meniscus, ligaments).

Numerical data given for the retrospective assessment of cartilage show an agreement of 36% to 100% [74]. The corresponding figures for meniscal lesions lie between 55 and 100% [58, 40, 70, 24].

It should be noted, however, that machines of different technical standards were used for the examinations. Moreover, the imaging of the cartilage with the gradient-echo technique requires that intraarticular fluid should be present, since it is this alone which makes it possible to achieve sufficient contrast for the demarcation of the cartilage surface.

Pathologic conditions investigated

Assessment of arthrosis

Advanced age need not necessarily be accompanied by gonarthrosis [21]. Casscells [10] was also able to demonstrate this in his investigation on 300 cadaver knee-joints.

The classification of Otte [56] has been used for the assessment of the histological and MR-arthrography findings. Otte distinguishes between four stages (Table 3.7).

This histological cartilage assessment is not directly applicable to the macroscopic assessment, however. The problems here concern the histological stages 1 and 2, because the structural change of the cartilage becomes manifest in a loss of the surface sheen (Table 3.7). The cartilage looks dull and appears of softer consistency than normal cartilage [34]. It is only in the advanced histological stage 2 and in stage 3 that circumscribed superficial defects appear macroscopically, seen as areas of roughness, unevenness or as deeper lesions.

The agreement between the histological and macroscopic findings is greatest in stages 3 and 4, since macroscopically extensive, focal cartilage defects and areas with complete loss of the cartilage, which have been described as bare bone [19] are present.

These stages have been correlated with the individual MR-images and the resulting therapeutic consequences have been indicated.

Normal cartilage

The macroscopically intact joint surface can be clearly demarcated on T1- and GE-images. The cartilage surface is defined by the contrast medium (Figure 3.1). The cartilage appears as an area of intermediate signal intensity. This can be demarcated from the subchondral zone on T1-weighted images through the high signal intensity of the bone marrow, which is rich in fat. The zone lying inbetween, which is of intermediate signal intensity, is made up of calcified and uncalcified cartilage and also of the subchondral bone plate. The zone of calcified cartilage is normally ca. 0.15 mm thick and lies above the uncalcified cartilage, demarcated by the tidemark. Together with the subchondral bone plate this results in a zone of 0.45 mm. Since this order of magnitude is still less

Table 3.7. Assessment of arthrosis with stage classifications

Histologic staging according to Otte [56]	Macroscopic staging	Radiographic staging according to Jonasch [39]	MR-arthrographic staging
Stage I Development of fine superficial fissures; loss of chondrocytes and proteoglycans	**Stage I** Loss of surface colouring (dull surface)		**Stage I** Surface normal Cartilage thickness normal
Stage II Fissures extending to subchondral zone "Cluster"-formation	**Stage II** Irregular cartilage surface with deep lesions, circumscribed defects	**Stage I** Slight narrowing of joint space (> 2 mm); degenerative loss of roundness and elongation of joint edges	**Stage II** Surface normal to slightly irregular; differences in cartilage thickness between T1 and GE
Stage III Loss of uncalcified cartilage; thickening of covering bone plate	**Stage III** Circumscribed cartilage defects; exposure of subchondral plate Bare bone	**Stage II** Joint space > 1 mm, marginal rim up to 5 mm wide	**Stage III** Irregular surface with defects up to bare bone, residual cartilage; differences between T1 and GE
Stage IV Opening up of subchondral medullary space. Granulation tissue. Regenerative fibrocartilage	**Stage IV** "Bare bone" dev. of regenerative tissue and fibrous replacement tissue	**Stage III** Joint space < 1 mm, marginal rim over 5 mm **Stage IV** Joint space < 0.5 mm Deformation of the joint surface	**Stage IV** Development of regenerative tissue Bare bone

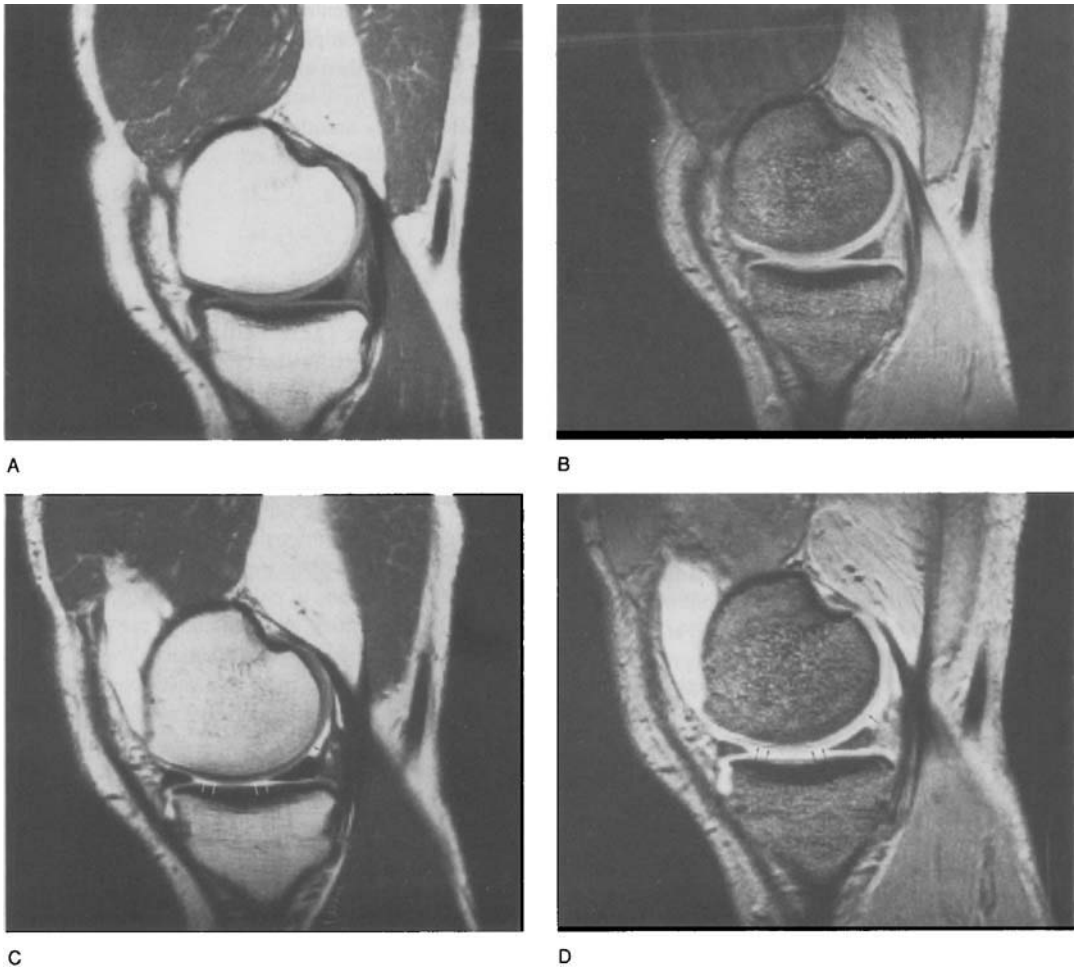

Figure 3.1. MRI, SE 700/15 (A+C), GE 30/10/30°, FISP-3D (B+D), normal knee-joint, sagittal plane, medial femoral condyle.

A and B. Before the intraarticular injection of Gd-DTPA.

C and D. After the injection.

The differentiation of the hyaline articular cartilage (arrow) applies to all sections of the joint, as long as sufficient contrast medium is present.

than the pixel size, this zone will make only an indirect contribution to the signal. On the GE-images the *zone of intermediate signal intensity* is caused exclusively by uncalcified cartilage tissue. The calcified part of the cartilage, the subchondral plate and the adjacent structures cannot be differentiated and display a uniform signal. Healthy cartilage will be visualised as being of approximately the same thickness on T1-weighted and GE-images.

Mild arthrosis

Signs of arthrosis are: changes in the form of a broadening of the subchondral bone plate, an increase in the zone of calcified cartilage [27] and often a doubling or several-fold increase in the tidemark [25]. This makes the cartilage appear thicker on T1-weighted images than GE-images (Figure 3.5).

The difference between the cartilage thickness seen on T1- and GE-images can therefore be interpreted as an indirect sign of structural cartilage changes. The broadening of the zone of calcified cartilage and the

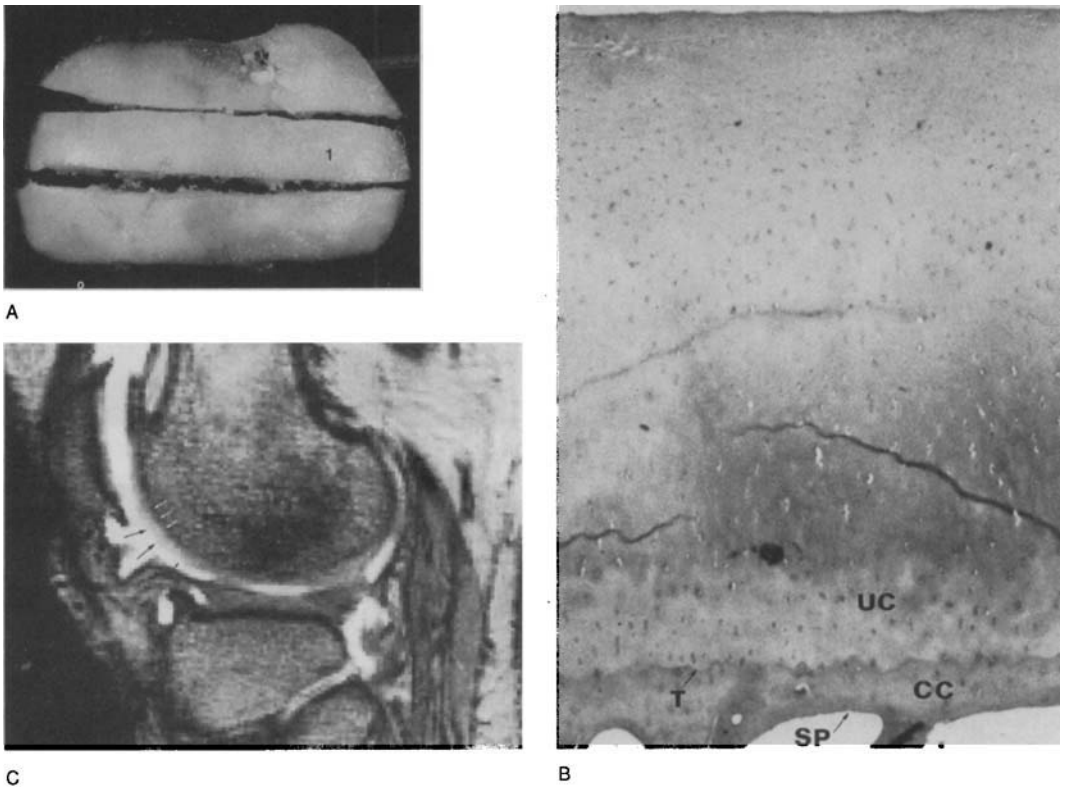

Figure 3.2. Mild arthrosis.

A. Macrograph. Central part of the lateral condyle, block taken for histologic investigations (1).

B. Structure of the hyaline articular cartilage and uncalcified cartilage (UC), tidemark (T), calcified cartilage (CC), and subchondral plate (SP) seen on light microscopy. HE, ×8.

C. GE 200/13/16, sagittal plane of middle section of the lateral condyle. Broad zone of inhomogenous intermediate signal intensity alongside a zone of low signal intensity (arrow).

several-fold increase in the tidemark occur early on during the processes of destruction in the cartilage, and are therefore already found in Otte's stage 1. (Figure 3.2).

A demasking of the collagen fibres (Figure 3.3), such as can occur in the course of arthrosis, can be detected as a structural change on MR-arthrography only if there are also changes in the calcified cartilage and the tidemark. If such changés are absent in the early stage, then the cartilage appears to be of the same thickness on both sequences.

The difference between the thickness of the cartilage which can be visualized in T1- and GE-images is the earliest sign of degenerative cartilage changes which can be detected by MR-arthrography. This sign supports the clinical diagnosis of a chondromalacia and helps to demonstrate it objectively.

Mild to moderate arthrosis (Figure 3.4). In MR-arthography the cartilage is visualized with a smoothly defined surface on both T1- and GE-images. Microscopically detectable fine fissure formations extending to the subchondral zone (Figure 3.4b) do not lead to any detectable changes in the signal of the cartilage. The fibrocartilage, resting on osteophytes, displays a low signal intensity on T1-weighted and GE-images. Only on GE-images is there a difference in the signal from hyaline cartilage, which shows an intermediate signal intensity (Figure 3.5).

This possibility of differentiation by MR-arthrography allows one to draw conclusions about the degree of the arthrosis.

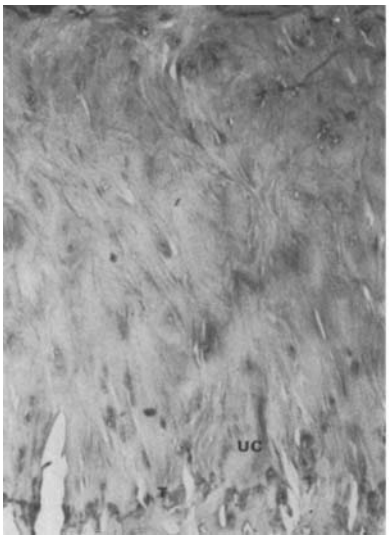

A

Figure 3.3. Mild arthrosis.

A. Histologic section. Demasking of the collagen fibres "asbestos fibres", tidemark (T), uncalcified cartilage (UC). HE, ×13.

B. MR-arthrography, SE 700/15, sagittal plane, ventral section of the condyle.

C. GE 30/10/30°, sagittal plane.

The zones of intermediate signal intensity corresponding to the cartilage show approximately the same thickness on T1- and GE-images (arrow).

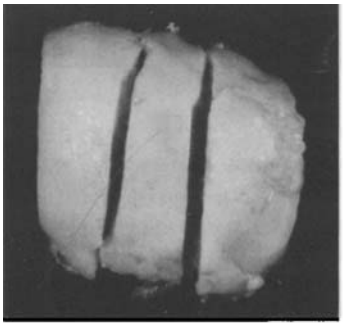

A

B

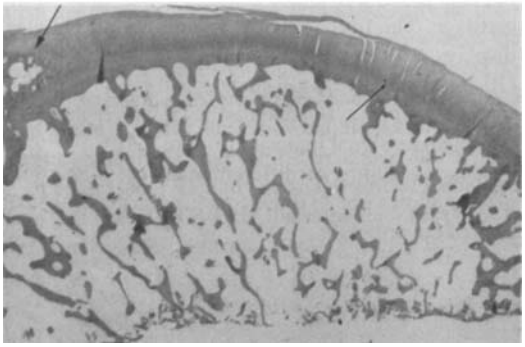

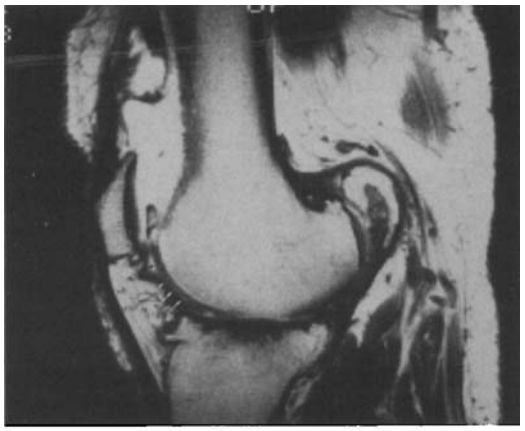

B

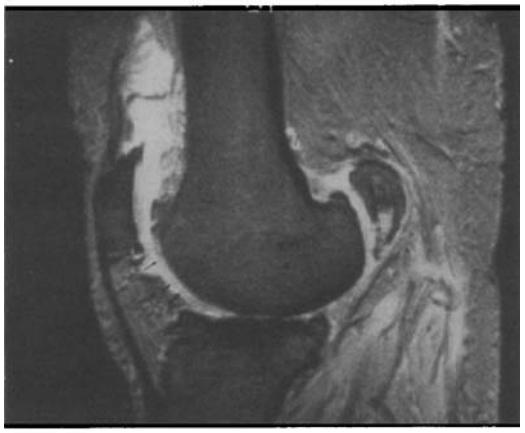

C

Figure 3.4. Moderate arthrosis.

A. Posterolateral section of a condyle, irregular cartilage surface sometimes with dull, but also with glossy, areas of cartilage.

B. Macrograph of a histologic section. Osteophyte in the posterior section of the condyle covered with fibrocartilage (arrow), old subchondral plate, development of fine cartilage fissures (arrow) extending to the subchondral plate. HE.

C. Microradiograph of the subchondral plate (SP), osteophytic new bone formation (OP).

C

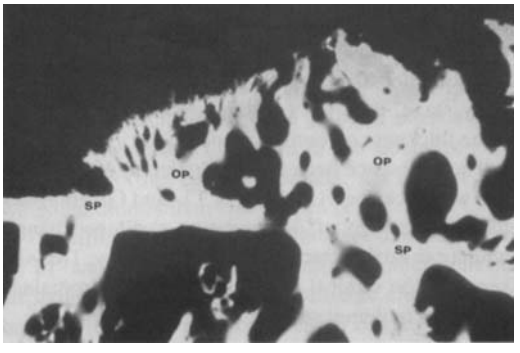

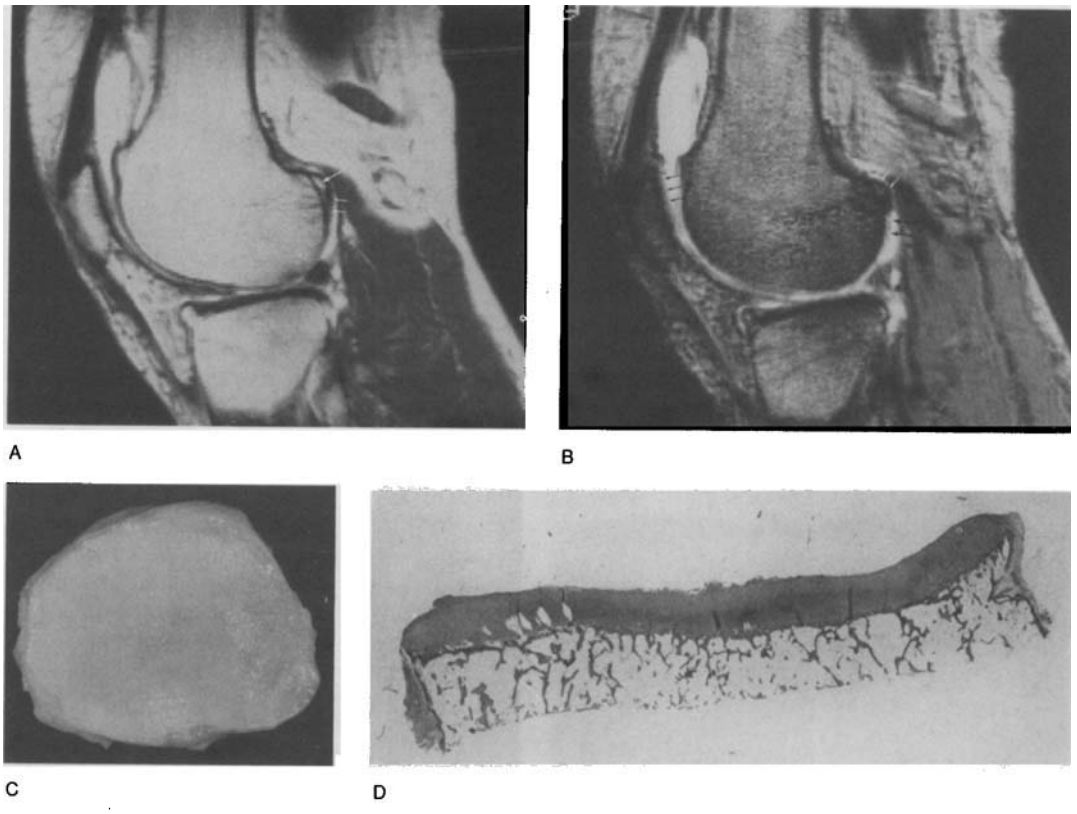

Figure 3.5. Moderate arthrosis.

A. MR-arthrography (SE 600/15, sagittal plane, posterior section of the condyle). Broad hypointense zone (arrow), which surrounds a signal-rich zone (osteophyte and fat marrow; arrow).

B. MR-arthrography (GE 30/13/35). Broad zone of intermediate signal intensity (arrow). Joint capsule extending up to the osteophyte. The osteophyte is surrounded by a zone of low signal intensity (arrow).
The fibrocartilage displays a low signal intensity, the hyaline cartilage an intermediate signal.

Patella. The cartilage appears broader on the T1-weighted images (A) than on the GE-images (B) because T1-images show both the calcified and the uncalcified cartilage, whereas GE-images show only the uncalcified cartilage.

C. Macrograph. The patellar cartilage surface is irregularly structured, slight marginal osteophyte formation.

D. Macrograph of the histologic section sagittally through the patella.

Severe arthrosis

Stage 3 (Figure 3.6). In MR-arthrography severe arthrosis is visualized by an irregular cartilage surface which is clearly demarcated by the contrast medium. The broadening of the zone of calcified cartilage and of the subchontral plate becomes apparent in an absolute reduction in the cartilage thickness and in the difference between the evaluable cartilage thickness on T1-weighted- and GE-images (see page 24). In our experience the assessment is reliable with a cartilage thickness of less than 1 mm.

Advanced Stages 3 and 4. In MR-arthrography the images in these stages are characterized by the absence of the intermediate signal intensities which are typical of the cartilage. This applies to both T1- and to GE-sequences (Figure 3.7). The assessment of the subchondral zone, up to the demarcation from the subchondral adipose tissue, is best achieved on T1-weighted images. On GE-images, good assessment of the surface is possible and subchondral cysts can also be detected. Osteophytes and degenerative meniscal changes can be visualized with both methods. The histological section picture shows that besides the ab-

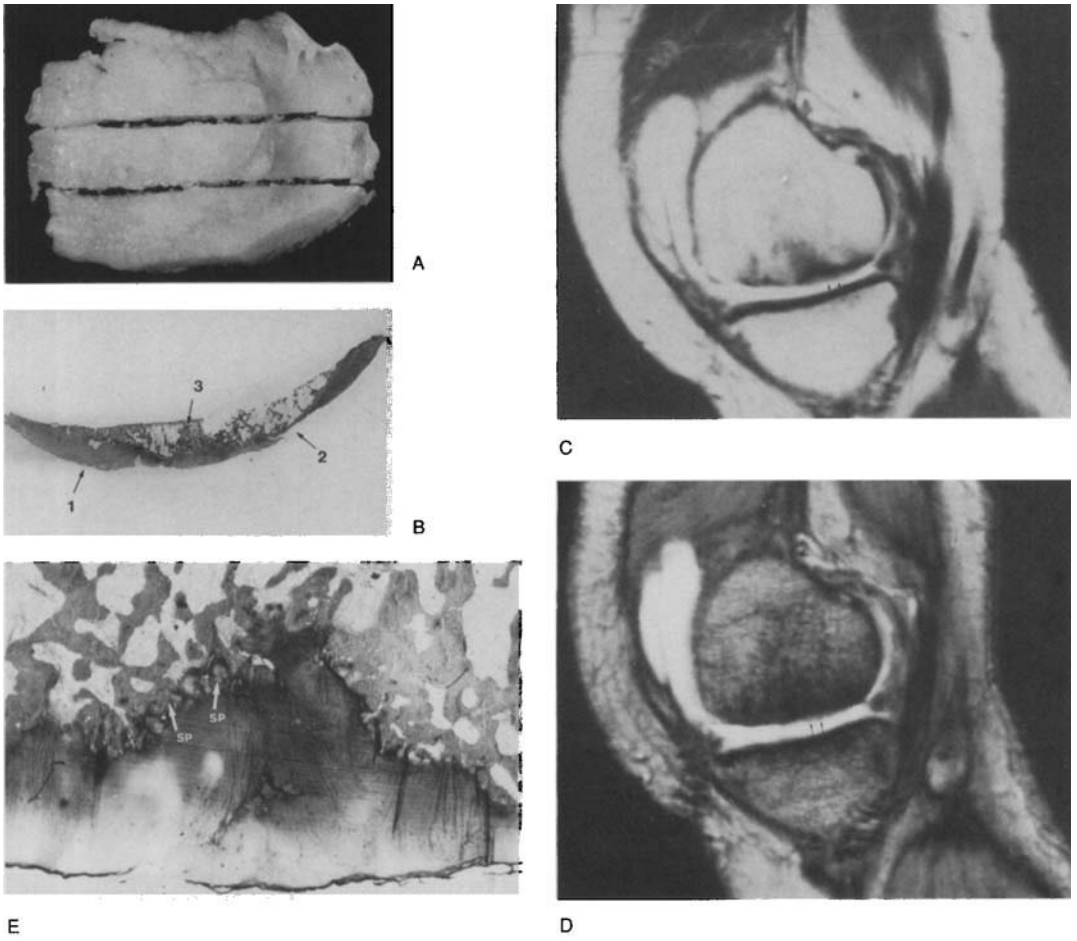

Figure 3.6. Severe arthrosis

A. Macrograph. Central section of the medial condyle. Irregular cartilage surface, sometimes with covering bone plate exposed, pseudo-regenerative granulation tissue.

B. Macrograph of a histologic section. Differences in cartilage thickness (zone with marked degenerative changes, area with absence of articular cartilage, cartilage-impressions). HE.

C. MR-arthrography (SE 600/15, sagittal plane). Focal area of cartilage (arrow), signal intensity of the adjacent subchondral space reduced. Somewhat irregular demarcation of remaining cartilage surface.

D. MR-arthrography (gradient-echo image, 30/13/35°). Distinctly narrowed focal area of cartilage with irregular surface.

E. Articular cartilage with few cells, broadening of the subchondral covering plate (SP), fairly high-grade degenerative cartilage changes. TB, ×2.6.

sence of cartilage, small areas of cartilage showing severe degenerative changes and cartilage-impressions may be present as well. Regenerative connective tissue is also found in the subchondral space and a very thickened covering plate. The changes described here become manifest on T1-weighted images as a linear hypointense subchondral zone.

It is not possible to differentiate between connective tissue, cartilage- and bone-dense areas on either T1- or GE-images. This is due to the cartilage volumes, which are in the order of magnitude of one voxel and the signals of which are reduced through partial volume effects, and also to the fact that this is cartilage which shows marked changes (few cells, rich in connective tissue). This brings about a signal

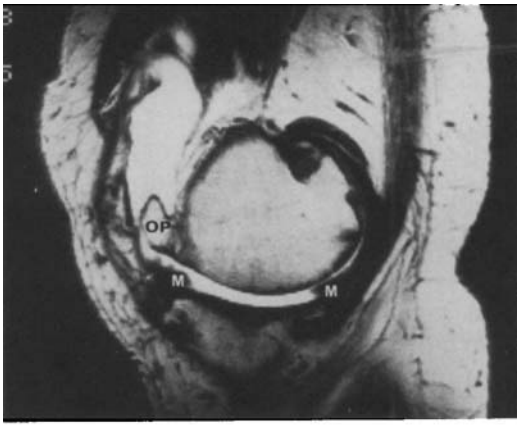

A

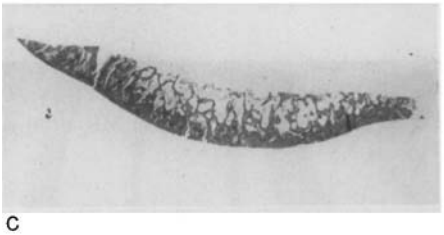

C

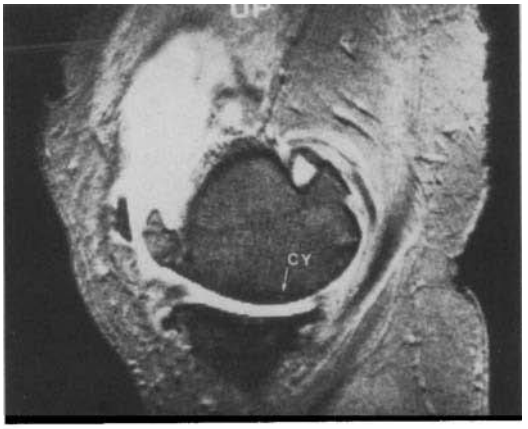

B

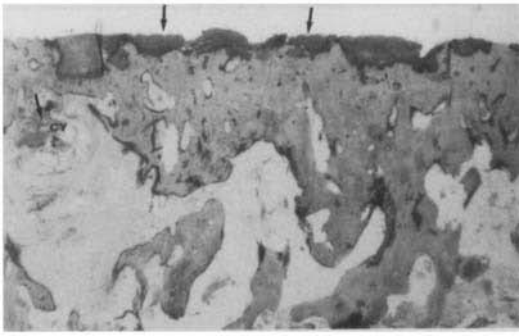

D

E

Figure 3.7. Severe arthrosis.

A. MR-arthrography (SE 700/15, sagittal plane of middle third of medial condyle). Smoothly defined condylar surface without articular cartilage, irregularly defined linear subchondral zones of hypointense signal intensity, large ventral osteophyte (OP) with signal intensity equivalent to fat, fragmented meniscus showing degenerative changes, fibrosed joint capsule (arrow).

B. MR-arthrography (GE 30/10/40°). Smoothly defined condylar surface without articular cartilage with small subchondral cyst (CY).

C. Macrograph of the histologic section. Smoothly defined condylar surface without articular cartilage. HE.

D. Cartilage remains showing high-grade degenerative changes, subchondral cyst (CY), cartilage-impression (arrow) surrounded by granulation tissue. HE, ×3.2.

E. Section of cartilage-impression. TB, ×16.

intensity identical to that of connective tissue and areas of sclerosis or of any hemosiderin deposits which may be present. The question of whether smooth bare bone and/or regeneration tissue are present is of great clinical interest. In the further course of events granulation tissue develops from the medullary space and also pseudoregeneration fibrocartilage tissue on the surface of the bone, denuded of cartilage (former subchondral plate).

Chondromalacia patellae

Chondromalacia patellae, defined as a localised lesion confined to the articular cartilage [28], cannot be distinguished histologically from arthrosis.

As already described for arthrosis, a limited assessment of cartilage damage is possible by MR-arthrography in stage 2 and an unequivocal assessment in stage 3. Intact cartilage surfaces and fine fissures or

Table 3.8. Comparison in chondromalacia between MR-arthrographic staging and the macroscopic staging of Outerbridge

MR-arthrographic staging	Macroscopic staging of Outerbridge
Stage I Surface normal, cartilage thickness normal **Stage II** Surface normal to slightly irregular; difference in cartilage thickness between T1 and GE	**Stage I** Local softening and swelling **Stage II** Fissures and fragmentation, lesions up to 1.3 cm in diameter
Stage III Irregular surface with defects up to "Bare bone"	**Stage III** As for Stage II, but lesions > 1.3 cm in diameter
Stage IV Development of regenerative tissue "Bare bone"	**Stage IV** Ulcers and erosions down to the bones

changes which are already macroscopically detectable (stage 1) do not become accessible, or only indirectly so, through the use of this investigation technique (Table 3.8).

Accurate visualization of the cartilage defect, its location and extent and also an assessment of the subchondral bone are possible by means of MR- arthrography (Figures 3.8–10).

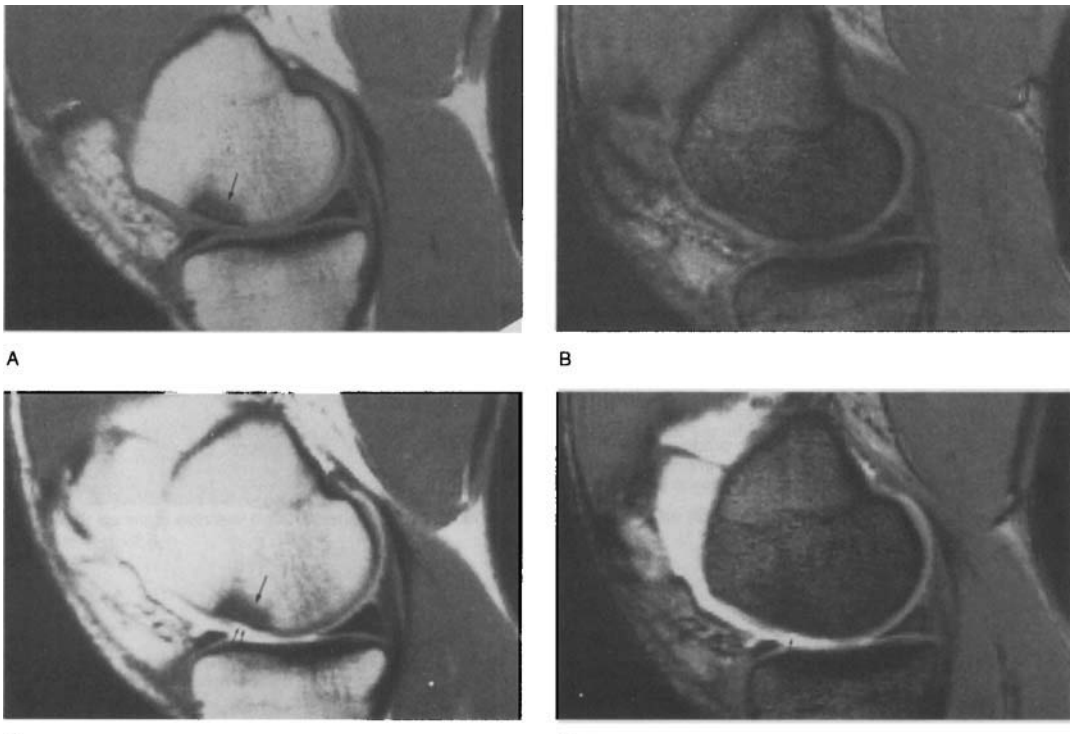

Figure 3.8. MRI, SE 700/15 (A and C), FLASH 300/15/135° (B and D). Chondromalacia of the medial condyle, sagittal plane, focal cartilage defect.

A and B. In the transitional region between the ventral and middle third of the medial condyle, circumscribed hypointense area extending into the subchondral cancellous bone (arrow).

C and D. MR-arthrography. Cartilage defect extending to the subchondral plate (arrow).

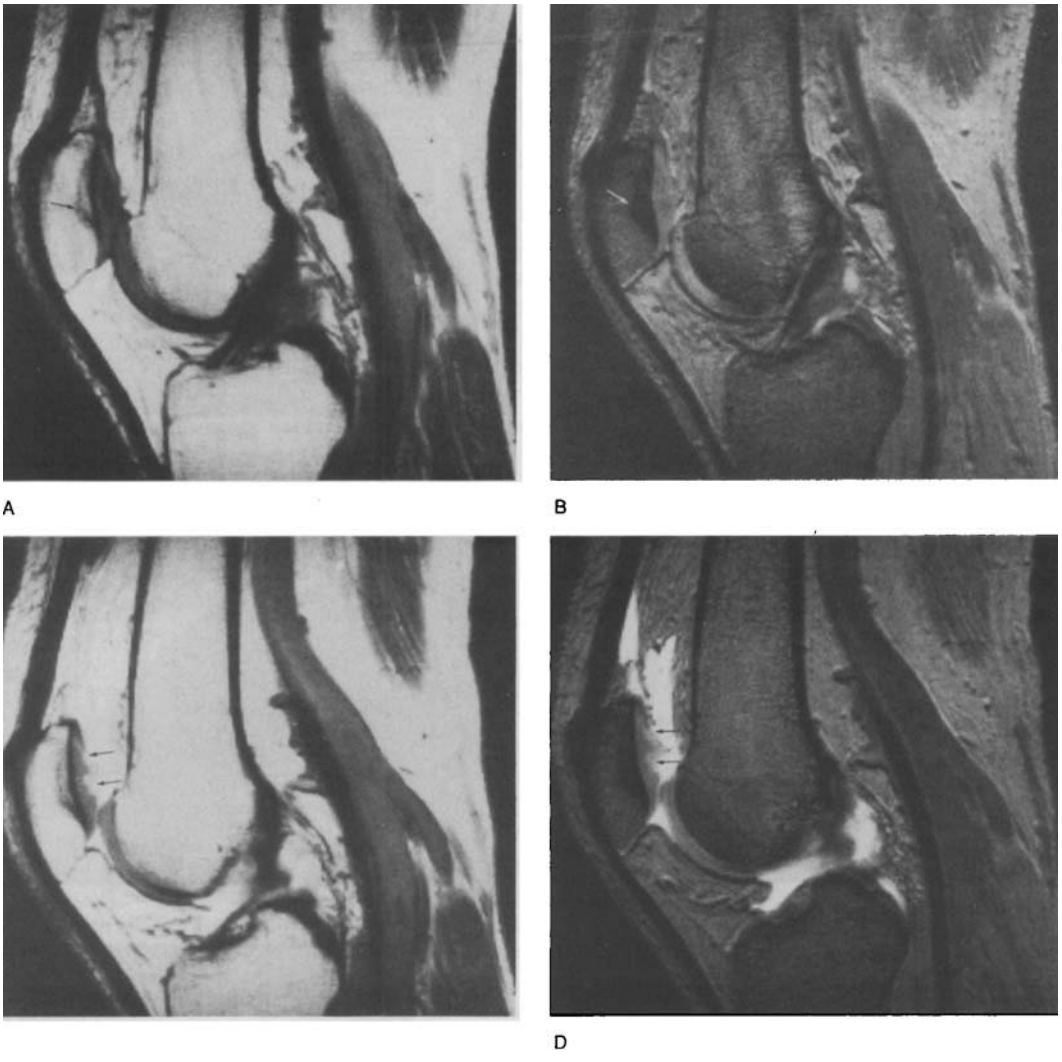

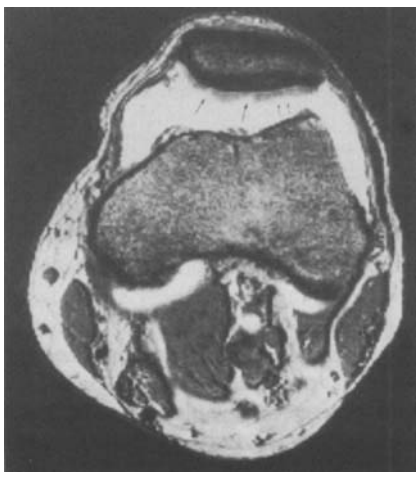

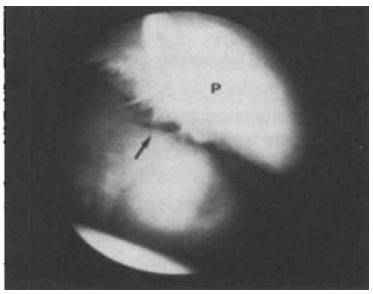

Figure 3.9. Chondromalcia patellae, sagittal plane, SE 700/15 (A and C), GE: 30/10/30° (B and D), GE: 30/10/30°, FISP-3D (E), axial section.

A and B. Articular cartilage of normal appearance, hypointense linear structure in the subchondral zone of the patella (arrow).

C, D and E. MR-arthrography. Irregular cartilage surface of the patella with multiple defects of varying depth (arrow).

F. Arthroscopy picture. Cartilage defect at the patella (P) in the form of fissures and villi (arrow).

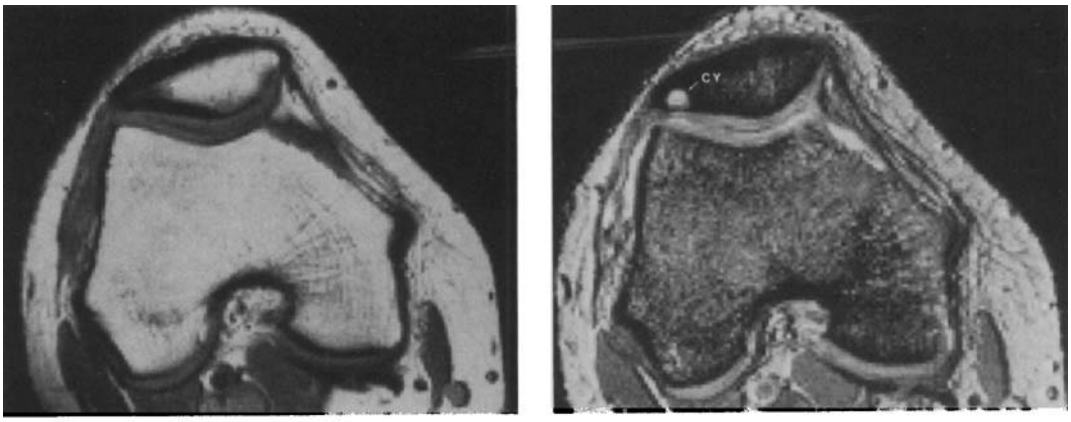

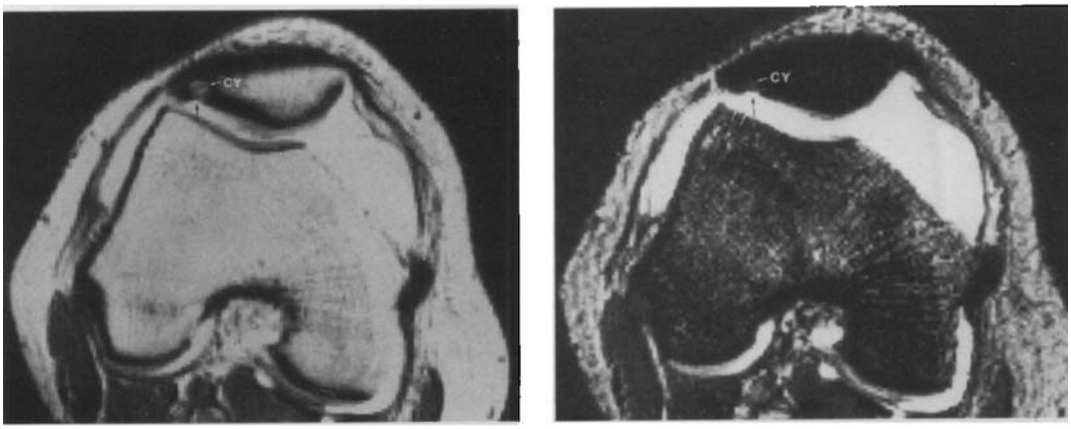

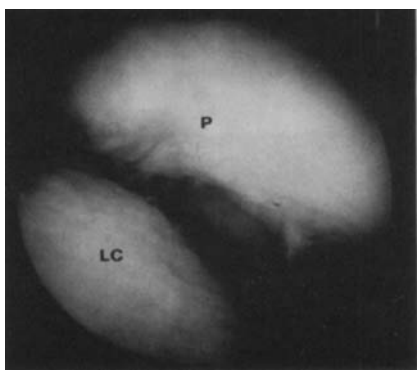

Figure 3.10. Patellofemoral condyle. Axial plane, SE 700/15 (A and C), GE 30/10/30° (B and D).

A and B. Cyst in the middle third of the lateral part of the patella

C and D. MR-arthrography. Focal cartilage defect, subchondral bone cyst (CY), narrow zone of cartilage at the hyaline cartilage of the lateral condyle opposite the defect (arrow).

E. Arthroscopy-picture. Focal cartilage defect with villi and fissures at the lateral patellar-surface (P). Roughening and irregular cartilage surface at the lateral condyle (LC).

Osteochondritis dissecans

The assessment of the location and extent of an osteochondritis dissecans is of decisive importance for the treatment [3, 43, 4, 5, 63, 15]. The following questions must primarily be answered:

1. Is a fracture of the cartilage present?
2. Is it a case of partial or total detachment of the fragments?
3. What are the characteristics of the bone layer?

The comprehensive diagnostic therapeutic algorithm of Clanton and De Lee [11] has been used to assess the image information, with the MR-arthro-

graphy findings being integrated into this scheme. The continuity of the cartilage surface and the degree of detachment of the fragments from the bone layer has been used as the main criterion of assessment for the determination of treatment. This results in a classification of the osteochondritis dissecans into 5 types:

Type 1: Intact cartilage surface, no line of demarcation, no separation, hypointense subchondral area which cannot be sharply demarcated (Figure 3.11).

Type 2: Intact cartilage surface, line of demarcation, early separation (Figure 3.12).

Type 3a: Partial cartilage fracture, dislocation of the detached fragments (Figure 3.13).

Type 3b: Partial cartilage fracture, dislocation of the detached fragments, subchondral cyst formation (Figure 3. 14)

Type 4: Total cartilage fracture, dislocation of the detached fragments (Figure 3.15).

Type 5: Loose body (Figure 3.16).

Table 3.9. Osteochondritis dissecans of the knee joint (n 16). Localisation and type according to MR-arthrography

Case	Age	Sex	Side	Localisation[a]	Type
S.F.	37	m	r	central	1
T.O.	26	m	r	central	2
T.O.	26	m	l	central	2
U.G.	19	m	r	anterior	2
K.J.	40	m	l	inferocentral	2
K.J.	40	m	l	inferocentral	2
M.N.	27	m	l	centrolateral	3A
M.A.	18	m	r	central	3A
M.N.	27	m	l	inferocentral	3A
U.G.	20	m	r	anterior	3A
K.J.	40	m	r	centrolateral	3A
K.T.	33	m	l	central	3B
K.J.	40	m	l	inferocentral	3B
S.D.	35	m	r	central	4
S.I.	22	f	r	loose body	5
F.S.	33	f	l	loose body	5

[a] Localisation according to Lindholm [15]

Fourteen osteochondral defects of sometimes differing location and also two loose joint bodies were classified in accordance with this system (Table 3.9).

An assessment of the cartilage surface or cartilage fractures without contrast medium was possible in 50% of the spin-echo images and in 29% of the GE-images (FISP 3D). This is reflected in the percentages for positive agreement in the comparison of the results with and without contrast medium. (T1:T1+Gd = 29%, T1:FISP+Gd = 36%, FISP 3D:T1+Gd = 36%, FISP 3D+Gd = 64%).

The existence of a cartilage fracture could be unequivocally demonstrated by means of MR-arthrography in both T1-weighted and also in FISP 3D-images or in the presence of a joint effusion. The best agreement was obtained between T1+Gd: FISP 3D+Gd at 93%, with the qualitative visualization of the fragments detached from bone being better on T1-weighted images and the cartilage being better visualized with FISP 3D plus contrast medium.

Guhl [29] and Ewing and Voto [18] have already pointed out the difficulties of assessing the cartilage surface by arthroscopy in osteochondritis dissecans, and they recommended staining with methylene-blue as an aid to the visualization of fine fracture lines or gradations, or reducing the strength of the light to improve the shadow-gradation.

Fissure formations in the cartilage and also the extent of the dislocation of cartilage and bone fragments are clearly visualized through the intraarticular use of the contrast medium. The combined view of the cartilage surface, the bone bed of the detached fragments and adjacent subchondral cancellous bone permits precise classification of osteochondritis dissecans

Hoffa's disease

Using MR-arthrography it could be demonstrated that the infrapatellar fatty body of Hoffa is not a homogenous structure but instead shows plicae and crypts. A healthy infrapatellar fatty body is always in contact with the femoral condyle in the region of the intercondylar fossa (Figure 3.17).

Hypertrophy of the infrapatellar fatty body could not be demonstrated, but rather a hypotrophy in cases where internal knee damage had been present for a fairly long time (arthrosis; Figure 3.18). This must be seen as part of a complex relationship since, besides the loss of contact with the femoral condyle surface one must at least take into account the anterior cruciate ligament, meniscal lesions and axial deformities as well. For the objective demonstration of disordered knee mechanics a straight line was drawn through the distal femur and the condyle in the sagittal median MR-arthrography section image (anterior and posterior cruciate ligament in one plane). This line always passed through the apex of the cuneiform condyle and intersected the plateau of the tibia precisely in the anterior margin of the origin of the ante-

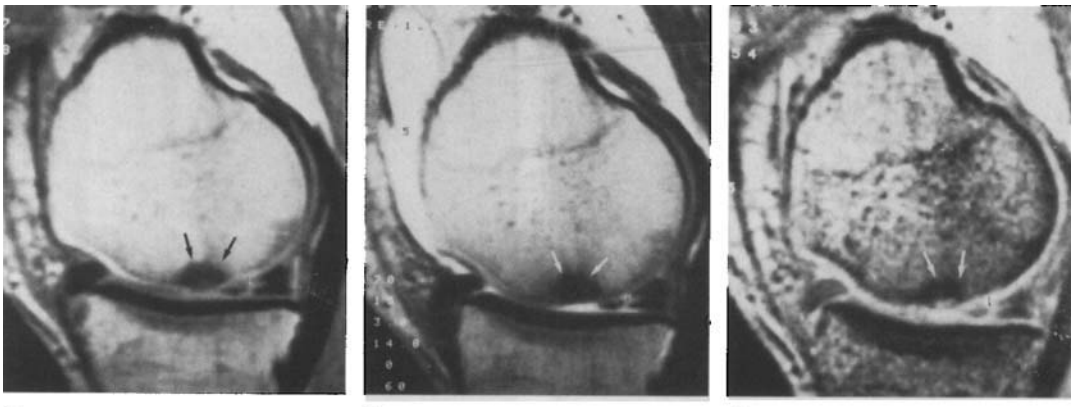

A B C

Figure 3.11. Osteochondritis dissecans Type 1. Sagittal plane, medial condyle, SE 700/15 (A and B), GE 30/10/30° (C and D).

A. MRI. The region of incipient osteochondritis dissecans is characterized by a subarticular zone of low signal intensity (arrow). Incidental finding: complete meniscal lesion in the medial posterior horn.

B and C. MR-arthrography. Intact cartilage surface (arrow), subarticular hypointense area (arrow). Entry of contrast medium into the complete meniscal tear (arrow).

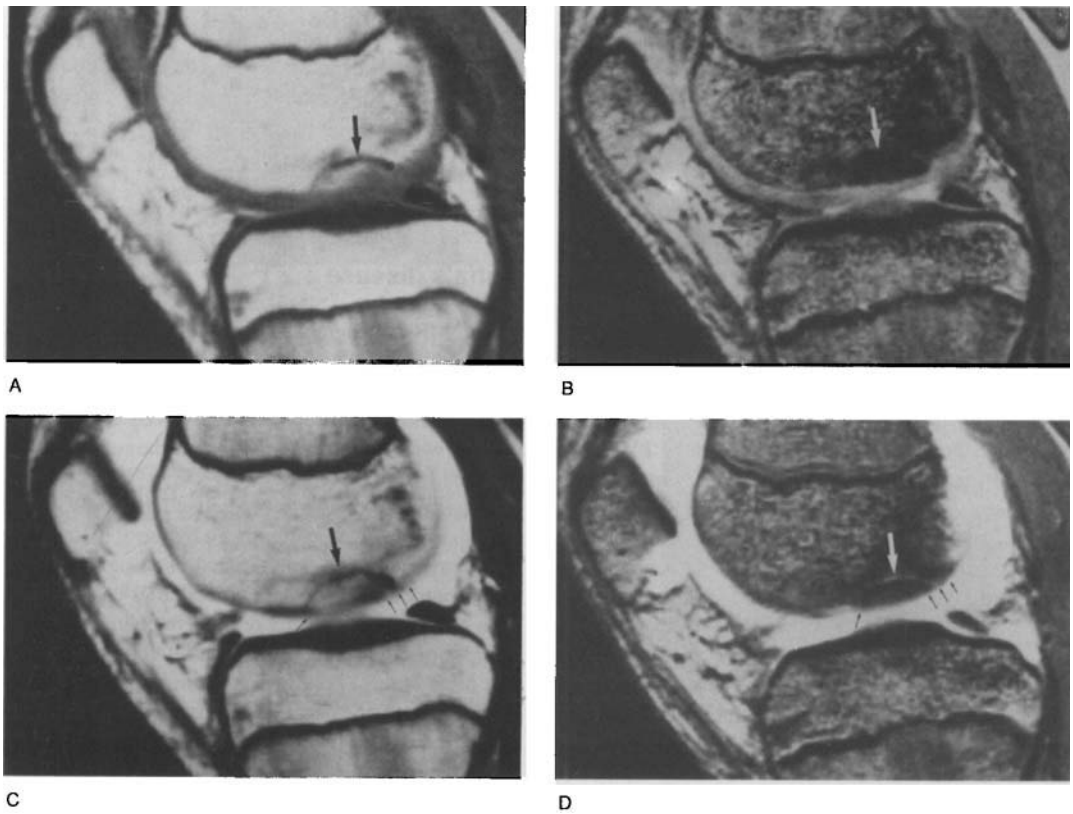

A B C D

Figure 3.12. Osteochondritis dissecans Type 2. Sagittal plane, medial condyle, SE 700/15 (A and C), GE 30/10/30° (B and D).

A. Distinct demarcation and early separation.

B. Ill-defined line of demarcation of the detached fragment.

C and D. MR-arthrography. Intact hyaline articular cartilage (arrows), demarcation of the detached fragment, and early separation (arrow).

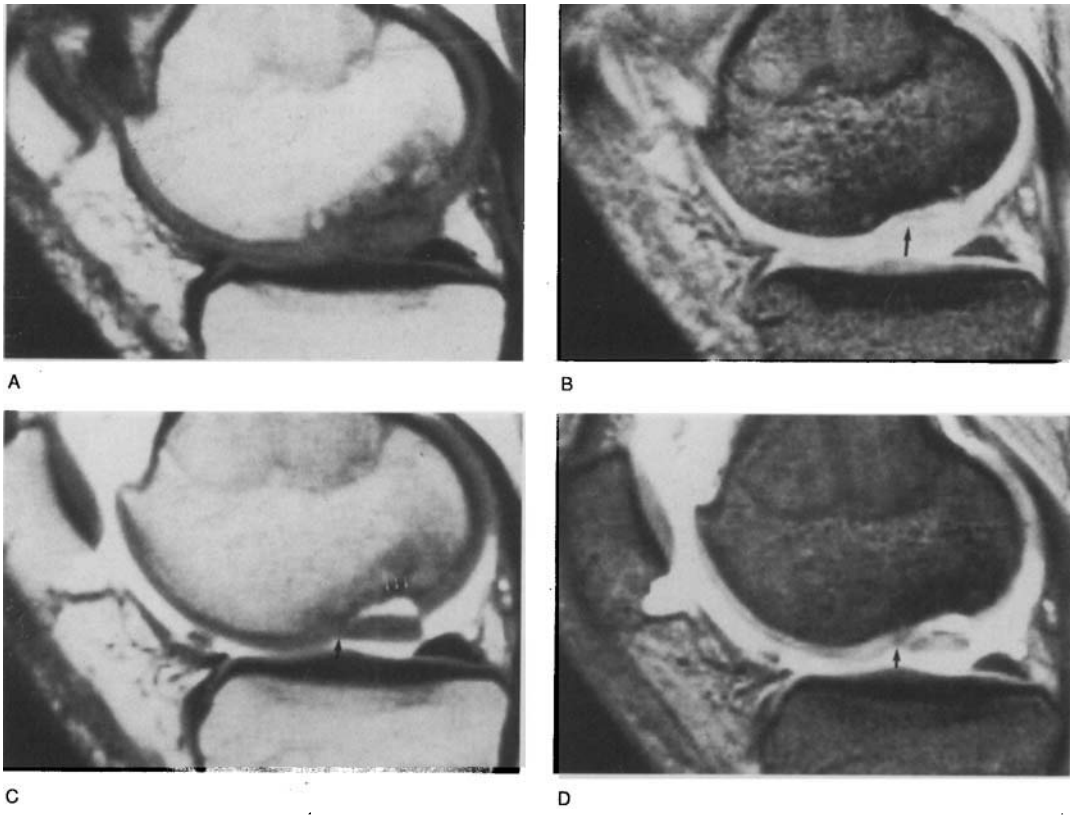

A B C D

Figure 3.13. Osteochondritis dissecans Type 3A. Partial cartilage fracture, dislocation of the detached fragment. Sagittal plane, medial condyle, SE 700/15 (A and C), GE 30/10/30° (B and D).

A and B. Formation of a defect in the joint-bearing middle third. The differentiation of the detached fragment is visible only on the GE-images.

C and D. MR-arthrography. The detached fragment is demarcated and is joined to the hyaline articular cartilage by a bridge of cartilage (arrow). Development of gradation due to a cartilage fracture. The hypointense zone in the defect layer (arrow) corresponds to a sclerosis of the subchondral bone.

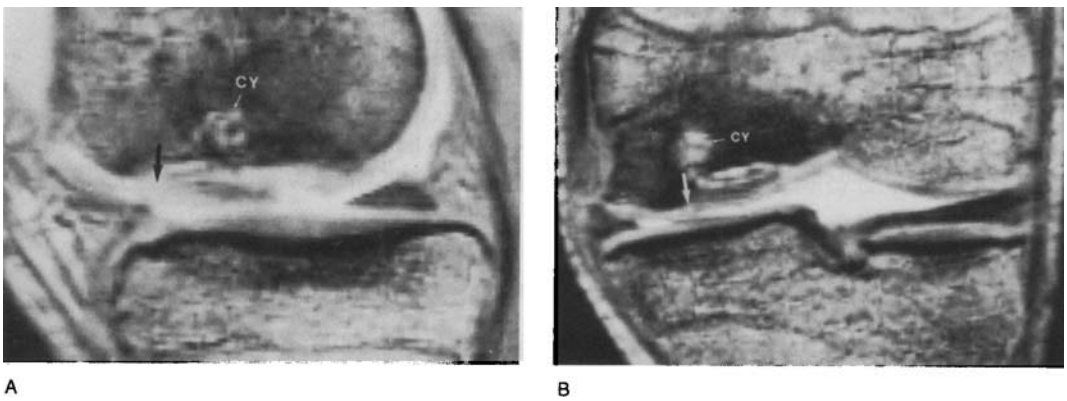

A B

Figure 3.14. Osteochondritis dissecans Type 3B. MR-arthrography (GE 30/10/30°). Sagittal plane, medial condyle (A) and axial plane (B).

A and B. Cartilage fracture with intact cartilage bridge (arrow), normal thickness of cartilage, dislocation of the detached fragment, bone cyst (CY).

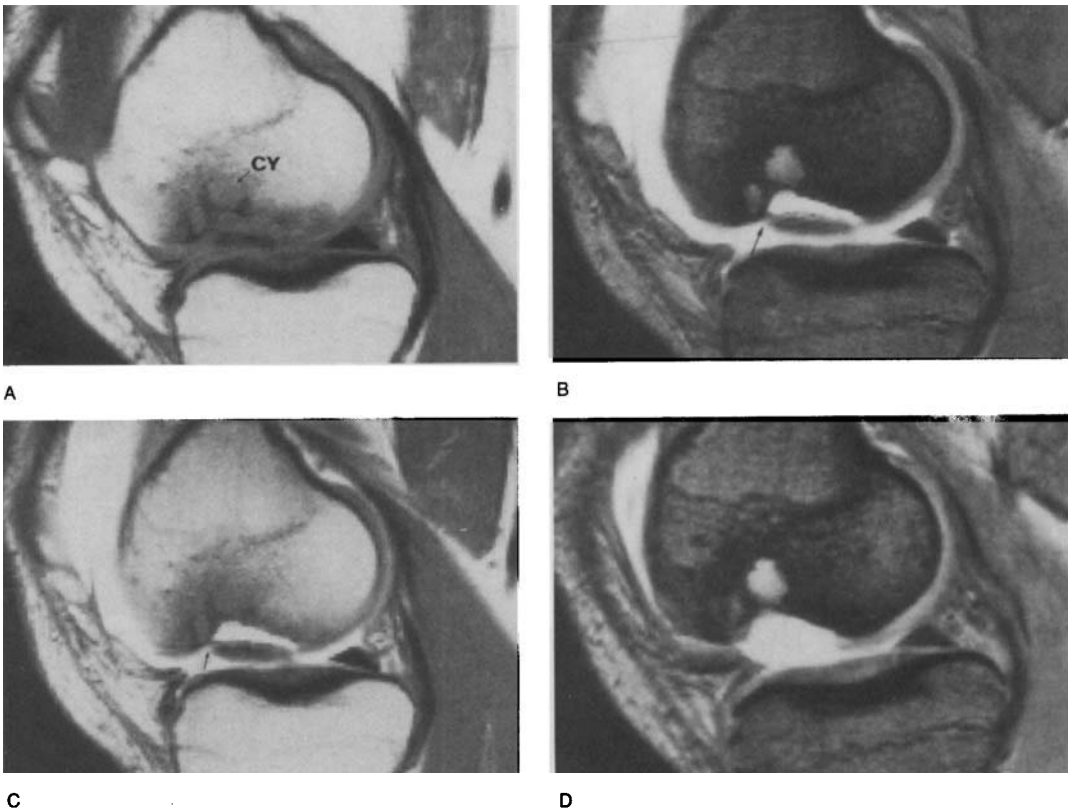

Figure 3.15. Osteochondritis dissecans Type 4. Sagittal plane, medial condyle, SE 700/15 (A and B), GE 30/10/30° (C and D).
A. Visualization of defect. No precise demarcation of detached fragment cyst formation (CY) in cancellous bone site of fragment.
B and C. MR-arthrography. Dislocation of detached fragment, complete cartilage fracture apart from a thin bridge of cartilage.
D. MR-arthrography. Site of detached fragment empty after total cartilage fracture and displacement of fragment.

rior cruciate ligament (Figure 3.19). The accurate visualization of this plane of section is not possible to any adequate extent without the use of contrast medium when fatty degeneration of the anterior cruciate ligament is present or after rupture of the anterior cruciate ligament.

Measurements of the distance between the tibial plateau and the femoral condyle showed (Table 3.10) that in the presence of a rupture of the cruciate ligament, distalization of the femur develops, and that if there are marked degenerative changes of the knee-joint, besides the distalization, ventralization or occasionally dorsalization of the femoral condyle also occur. This means that the apex of the femoral condyle comes to lie on the tibia before/behind the insertion of the anterior cruciate ligament (Figure 3.20).

Table 3.11. Relative displacement of the joint surfaces of the femoral condyle and tibia as a result of loss of function of the anterior cruciate ligament. Mean *SD* (Range)

	Normal knee joint (n 19)	Ruptured anterior cruciate ligament (n 3)	Arthrosis[a] (n 10)
Distalization	1.0 *0.2* (0.8–1.4)	0.6 *0.3* (0.6–0.7)	0.5 *0.1* (0.2–0.6)
Ventralization	none	none	0.4 *0.7* (1.0–1.4)

[a] Arthroses Grades III and IV according to Jonasch [39].

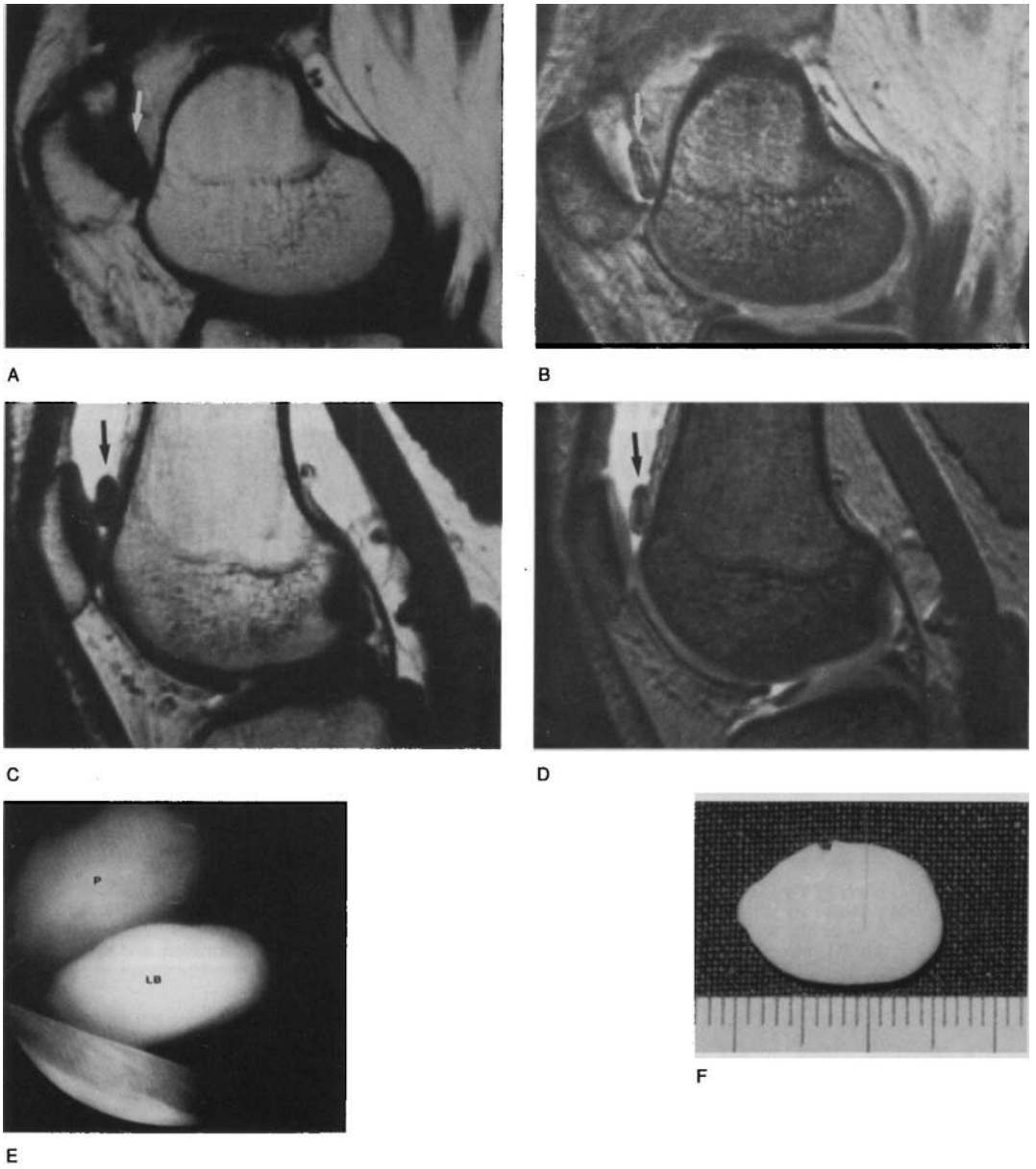

Figure 3.16. Osteochondritis dissecans Type 5 with loose body. Sagittal plane, SE 700/15 (A and C) GE 30/10/30° (B and D).

A and B. Loose joint body lying in the upper recess (arrow).

C and D. MR-arthrography. Distinct demarcation of the loose joint body, central ossification surrounded by broad areas of cartilage (arrow).

E. Arthroscopy picture. Loose joint body (LB), patella (P).

F. Photograph of the loose joint body.

This is associated with a loss of contact of the infrapatellar fatty body and possibly distalization of the patella and also a change in the surface contact between the patella and the femoral condyle. This becomes manifest in the development of osteophytes and degenerative cartilage changes.

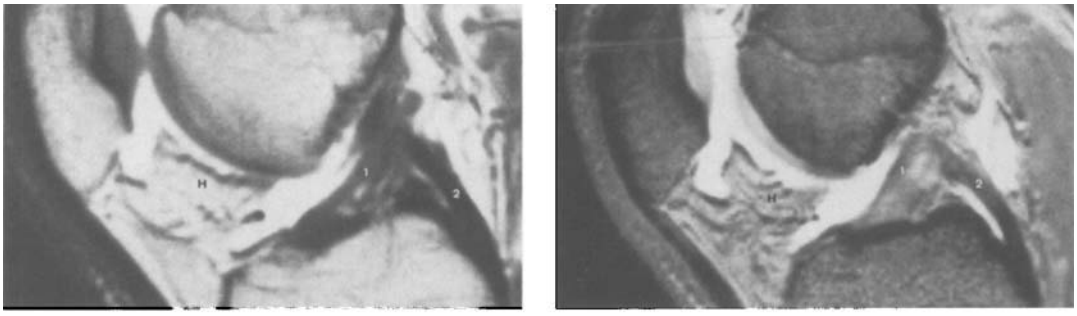

A B

Figure 3.17. MR-arthrography, SE 700/15 (A), GE 30/10/30° (B), sagittal-median section. Broad, linguiform area of contact between the infrapatellar fatty body of Hoffa (H) and the condyle, distinct demarcation of the cruciate ligaments by the contrast medium. Anterior cruciate ligament (1) and posterior cruciate ligament (2).

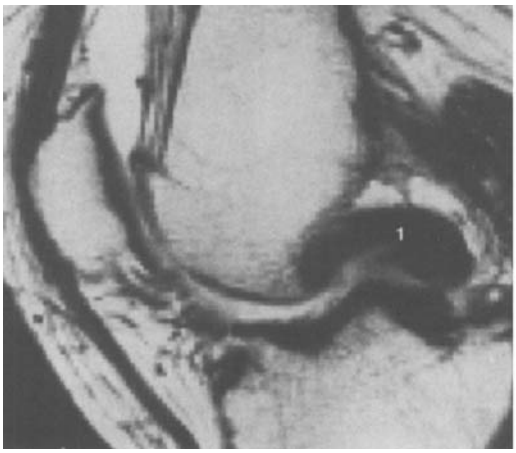

Figure 3.18. MR-arthrography (SE 700/15, GE 300/10/135°, FLASH-2D, sagittal plane). Hypotrophy of the infrapatellar fatty body of Hoffa, absence of anterior cruciate ligament, posterior cruciate ligament (1), arthrosis, distalization and ventralization of the femur.

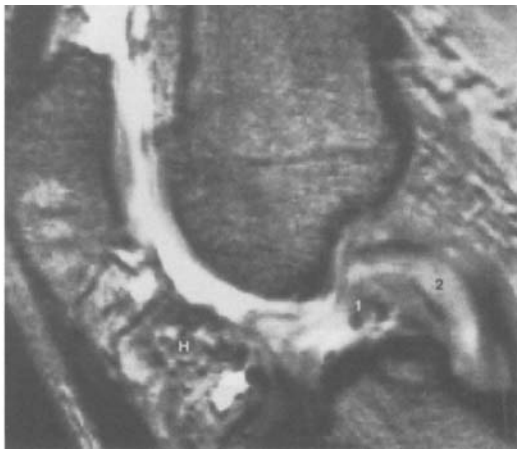

Figure 3.19. MR-arthrography (GE 30/10/30°). State after reconstructive surgery of the cruciate ligament. Rupture of the anterior cruciate ligament. Cruciate ligament stump (1), posterior cruciate ligament (2), crypt-formation, and hypotrophy of the infrapatellar fatty body of Hoffa (H).

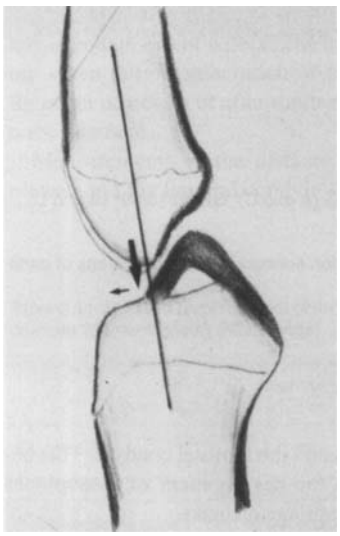

Figure 3.20. Illustration of possible distalization and ventralization (arrows) in the absence of the anterior cruciate ligament.

Plica-syndrome (shelf-syndrome)

Of all the folds which are ontogenetically possible in the knee-joint, (plica suprapatellaris, mediopatellaris and infrapatellaris) the plica mediopatellaris is of the greatest pathological importance. Good visualization of the plica suprapatellaris (Figures 3.21–22) and plica mediopatellaris (Figures 3.23–24) is possible by MR-arthrography.

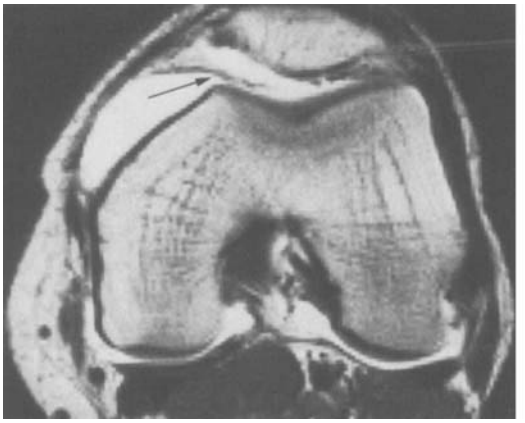

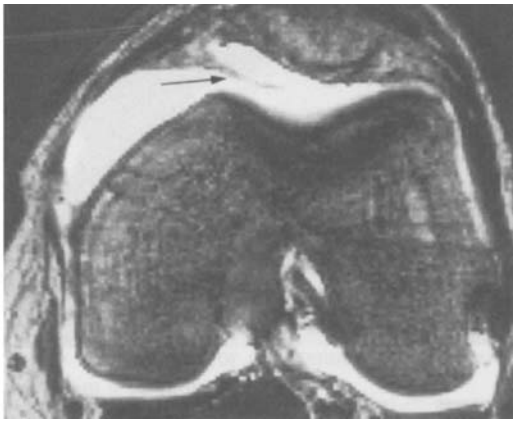

Figure 3.21. MR-arthrography, SE 700/15 (A), GE 30/10/30° (B), axial plane. Plica mediopatellaris (PM) stretched out between the patella and the medial condyle. Type C according to Iino: large "sail", which covers the anterior part of the medial condyle (arrow).

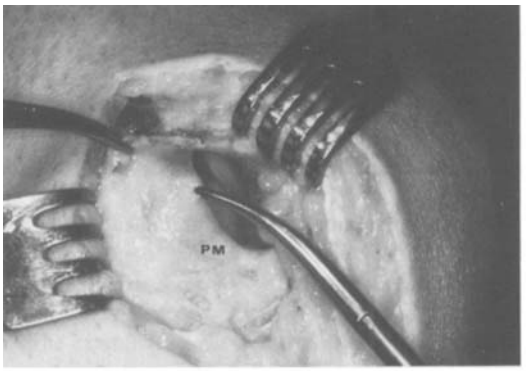

Figure 3.22. Macrograph. Plica mediopatellaris (PM).

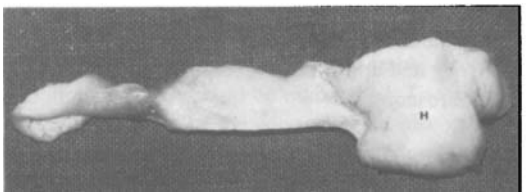

Figure 3.24. Macrograph. Resection specimen. Plica mediopatellaris extending from the infrapatellar fatty body of Hoffa (H) up to the plica suprapatellaris.

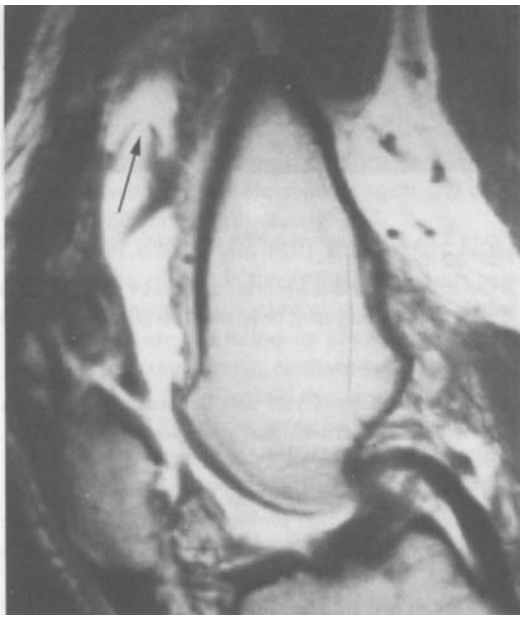

Figure 3.23. MR-arthrography, SE 700/15 (A), GE 30/10/30° (B), sagittal plane. Plica suprapatellaris: the septum suprapatellar (arrow) shows a central perforation site, which is called the porta.

Lesions of the meniscus

Magnetic resonance imaging ... h degree of accuracy in the diagnosis of le ... meniscus [40, 67, 73, 58]. On T1-weighted ... ibrocartilage of the meniscus appears to be of homogenous structure with a very low signal intensity [49, 72, 70, 60, 61, 14, 15, 23, 41]. Any pathological change will result in an increase in the signal intensity on T1-weighted images. Thus meniscal tears appear as linear increases

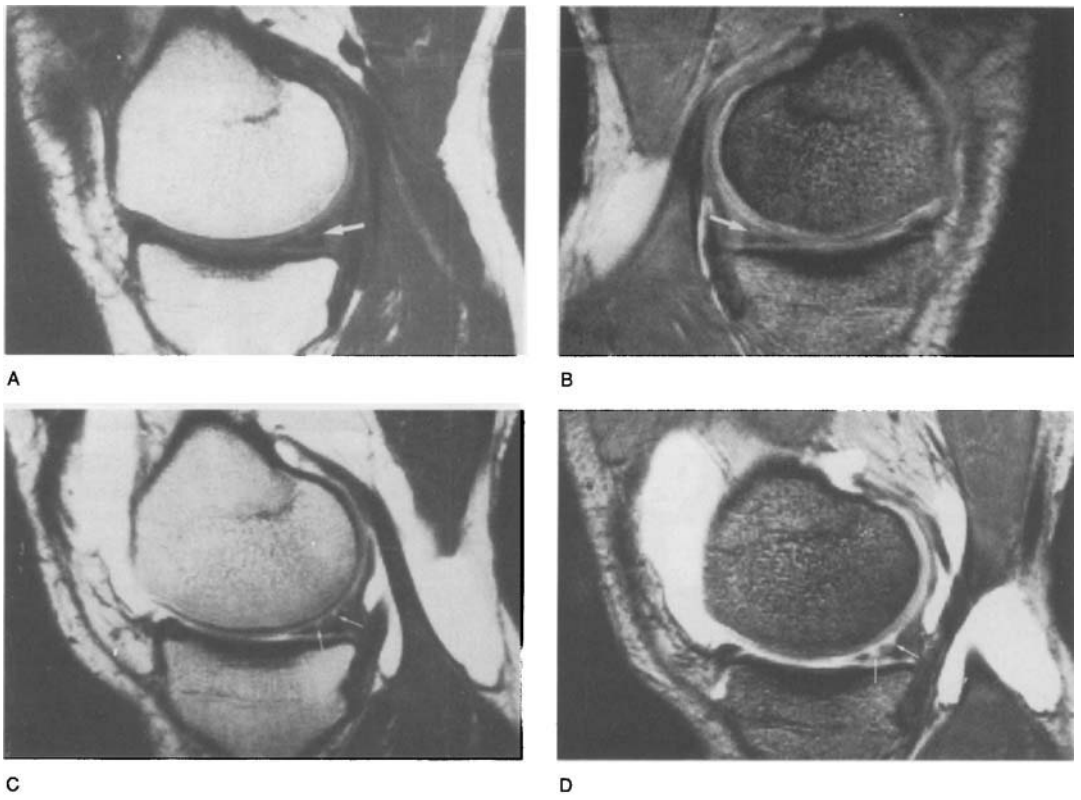

Figure 3.25. Partial tear of medial meniscus. Sagittal plane through the medial condyle, SE 700/15 (A and C), GE 30/10/30°, FISP-3D (B and D).

A and B. Inhomogenous signal in the posterior horn (arrow), evidence of a meniscal lesion.

C and D. MR-arthrography. Small meniscal tear (arrow) identified by the contrast medium.

in signal intensity. Cysts and degenerative changes lead to a circumscribed increase in signal intensity inside the meniscus [6, 14, 45, 46].

The detection of tears in menisci showing degenerative changes is often problematical however, since both of these lead to an increase in the signal which can reach that of intraarticular fluid [72].

Through MR-arthrography the contours of the menisci can be accurately defined, regardless of whether degenerative changes are present or not (Figure 3.25). Even small superficial tears can be visualized and it can be determined whether a tear extends to the surface. If the contours of the meniscus appear intact, it can be demonstrated that an intrameniscal tear is present.

Conclusions

1. MR-arthrography is characterized by high sensitivity and specificity—comparable with those of arthroscopy.

2. Both the surface and also osseous parts of the joint can be assessed through this method.

3. Pathological changes can be visualized to a greater extent after the intraarticular administration of contrast medium.

4. Clinically, the use of the method is mainly indicated: a) for the diagnosis of uncharacteristic pain in the knee-joint; b) to determine the degree of severity of pathological cartilage changes; c) possibly to monitor the course of such pathological change; d) when there are medical contraindications to arthroscopy.

Summary

This study contains the fundamentals and the technique of the intraarticular application of an MRI contrast agent in connection with magnetic resonance imaging (MRI arthrography). It also presents the resulting clinical relevance for knee joint diagnostics.

The significance of MRI arthrography is linked above all to the central question of whether or not it is possible to depict the hyaline cartilage, its surface and its thickness with the help of MRI arthrography.

MRI arthrography was used for in vitro examinations of rabbit knee joint cartilage and human joint cartilage. The in vivo application was carried out in 73 patients.

Apart from the metric evaluation and the assessment of the information content of the MRI image, the corresponding histologic sections were made in 20 knee joints in order to compare the cartilage surface and the thickness of the cartilage with the results in the MRI image. The optimum amount of contrast agent for visualization was determined, the uptake and clearance of the contrast agent from the cartilage were assessed, and trace elements from the cartilage were also analyzed.

The examination showed that the molecular structure of the contrast agent (gadolinium-DTPA) does not prevent the uptake of the contrast agent into the matrix of the hyaline cartilage. But this process is reversible. Thus, 14 hours after the intraarticular application of the contrast agent no measurable traces of gadolinium-DTPA could be established. The intraarticular application of the contrast agent also made it possible to achieve a constant and reproducible visualization of all joint structures. This affected mainly the surface of the hyaline cartilage.

The best imaging quality was achieved with intraarticular application of 30 to 40 mL of a 2 mmolar solution of gadolinium-DTPA.

The technique used for the intraarticular application is the same as for the common procedures of knee joint aspiration.

The clinical importance of MRI arthrography lies in the fact that a very detailed assessment can be made for therapy planning and furthermore in the possibility to provide the surgeon with answers to specific questions concerning the therapy. Examples are the extent and location of chondromalacia in a patient and the question whether a cartilage fracture has already occurred in osteochondrosis dissecans or not. The evaluation of cartilage together with the possibility to assess all other structures in the knee joint is a special feature of MRI arthrography. The high sensitivity and specificity of this method makes it superior to the examination without contrast agent and comparable to diagnostic arthroscopy.

The main emphasis of MRI arthrography in the clinical application is in the evaluation of knee pain with an uncharacteristic clinical appearance. Other possible uses are the follow-up after surgical interventions, for example after cartilage-bone grafts.

In summary, it can be said that the contrast agent gadolinium-DTPA for the intraarticular application in MRI arthrography can achieve an optimum visualization of the hyaline joint cartilage. This method is therefore an important addition to the range of diagnostic measures for the knee joint.

Acknowledgements

My special thanks are due to Prof. Dr. R. Kotz, my academic mentor and Head of the Department of Orthopedics, University of Vienna, and to Prof. Dr. H. Imhof, Head of the Magnetic Resonance Institute, University of Vienna, who afforded me the possibility to explore the use of magnetic resonance arthrography in clinical practice.

Special thanks I owe to the Schering Corporation for their generous contribution to the printing costs.

Acknowledgement is also due in particular to the Vienna Academy of Postgraduate Medical Education and Research with Dr. D. Fleischmann who composed the manuscript and designed the graphics, to Ms Inge Wolfarth who was the photographer and to Mr. Jäger who did the layout of the photographic material.

Appendix 1. Resection areas for the histochemic and histologic evaluation

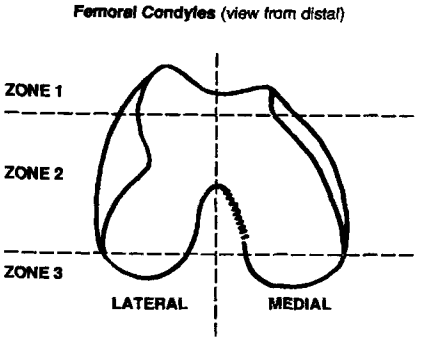

Appendix 2. Average Relative Volume Density (vVol%) of the cancellous bone with osteoid tissue located directly adjacent to cortex or below cartilage (2 zones, dimension of grid 2 x 2 mm)

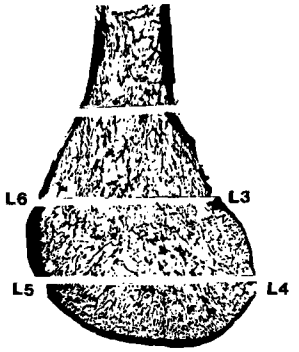

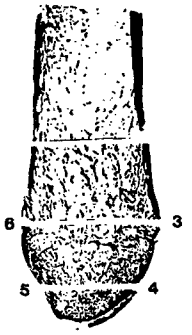

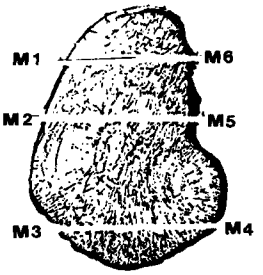

Lateral (L)

L3 - L4:
Zone 1: 16, 16, 22, 11, 11, 33, 11, 13, 22
Zone 2: 11, 16, 11, 11, 11, 16, 11, 16, 13

L4 - L5:
Zone 1: 22, 22, 38, 25, 22, 22, 27, 36, 30, 36, 34, 34, 34, 34, 24, 24, 24, 32, 32, 28, 28, 30, 28, 28, 36, 42
Zone 2: 19, 11, 16, 25, 16, 24, 24, 24, 23, 23, 23, 24, 23, 23, 23, 23, 25, 25, 25, 25, 23, 23, 23, 23, 23

L5 - L6:
Zone 1: 19, 16, 13, 27, 22
Zone 2: 22, 16, 16, 16, 11, 19, 11

Median (Med)

Med3 - Med4:
Zone 1: 33, 30, 30, 52, 55, 61, 50, 41
Zone 2: 22, 11, 33, 33, 16, 19, 44

Med4 - Med5:
Zone 1: 47, 41, 41, 25, 27, 30, 19, 38, 22, 36, 38, 36
Zone 2: 33, 17, 19, 30, 25, 36, 38, 44, 38

Med5 - Med6:
Zone 1: 30, 25, 30, 30, 22, 33
Zone 2: 22, 30, 33, 22, 27, 38

Medial (M)

M1 - M2:
Zone 1: 11, 5, 5, 11, 8, 8
Zone 2: 3, 11, 5, 13, 8, 13

M2 - M3:
Zone 1: 33, 27, 16, 19, 36, 30, 16, 27, 16, 25, 27, 25, 19
Zone 2: 16, 11, 25, 11, 16, 19, 19, 16, 13, 19, 27, 19, 5

M3 - M4:
Zone 1: 41, 38, 55, 47, 47, 25, 16, 32, 36, 36, 36, 38, 27, 33, 30, 22
Zone 2: 19, 16, 25, 33, 36, 33, 41, 30, 30, 36, 38, 25, 19, 16

M4 - M5:
Zone 1: 11, 13, 22, 13, 8, 11, 8, 19, 13, 16, 19, 36
Zone 2: 11, 16, 11, 11, 11, 13, 13, 5, 19, 13, 27, 25

M5 - M6:
Zone 1: 30, 27, 30, 22, 33, 29
Zone 2: 25, 36, 16, 22, 25, 44

M6 - M1
Zone 1: 27, 13, 50, 16, 13, 13, 30, 13, 13, 22, 33
Zone 2: 27, 16, 13, 27, 19, 16, 11

Appendix 3. Summary of MR findings (T1, GE, T1-Gd, and GE-Gd) of patients with knee joint symptomatology. (N 53)

Case	Cartilage	Meniscus	Synovitis	Cruciate lig.	Osteochondritis	Loose body	Spongy bone
O.N. 20 w	CL						
K.W. 60 m	CM CM		E E S S				
K.M. 28 w	CP CP		PM PM				MC MC MC MC
J.R. 68 m	CM CM	M M M M	S S				MC MC MC MC
T.A. 24 m							
W.M 27 w	CM		S S S S	A A A A			LC LC LC LC
B.G. 29 m							
St.I. 22 w	CM		S S			LB LB LB LB	
H.K. 34 m	CP CP CP CP	M M M M					
B G. 49 m	CL	L L L L					
K.H. 27 m							
K.C. 20 m	CL CL		PS PS				
G.J. 30 w	CM CM		PS PS				MC MC MC MC
G.H. 35 m		M M M M					MC MC MC MC
W.G. 35 m							
F.E. 47 w	CP CP CP						C C C C
L F. 18 w			PS PS				
H.M. 28 m		LM LM					
S.D. 35 m					OC OC OC OC	LB LB	MC MC MC MC
S.V. 31 w							
S.S. 20 w			E E S S				
G F 55 m	CP CP	M M M M					
W E 37 w				A A A A			MC MC MC MC
W W. 34 m		M M M M					
V.G. 19 m	CP CP				OC OC OC OC		LC LC LC LC
T.A. 55 w	CM CM						MC MC MC MC
	CP CP						
F.S. 33 w	CM CM					LB LB LB LB	
	CP CP						
B.N. 16 m							
K.J. 40 m	CM CM						MC MC MC MC
	CL CL				OC OC OC OC		LC LC LC LC
K.J 40 m							
E.G. 17 m				A A A A	OC OC OC OC		
H.F. 45 m			PS PS				
K.K. 13 w							
G.N. 14 m							
L S. 27 w		M M M M	PS PS				
L.K. 25 m	CP CP CP CP	M M M M	S S S S	A A A A			
H.K. 46 m		M M M M					
W.H 37 m							
F.A. 40 m							
S.R. 23 m							
M.N. 27 m	CL CL CL CL	L L L L	S S S S				LC LC LC LC
	CM CM CM CM						
M A 18 m	CM CM				OC OC OC OC		
T.O. 26 m			PS PS		OC OC OC OC		MC MC MC MC
P.E. 34 w	CP CP						LC LC
							P P P P
F.W. 72 m	CP CP CP	M M M M	E E S S	A A			P P P P
	CM CM						MC MC MC MC
T.O. 26 m					OC OC OC OC		MC MC MC MC
T.O. 26 m					OC OC OC OC		MC MC MC MC
M.A. 18 m	CM CM				OC OC OC OC		MC MC MC MC
F.W. 72 m	CM CM CM CM						LC LC LC LC
	CL CL CL CL	M M M M					MC MC MC MC
	CP CP CP CP	L L L L	E E S S				
P.E. 34 w	– – CP CP		– – S S			LB LB LB LB	P P P P
			PS PS				
S.M 21 m			PS PS				
S.F. 37 m	CM	M M M M	E S S		OC OC OC OC		MC MC MC MC
K.T. 33 m	CM CM CM CM	M M M M			OC OC OC OC	LB LB LB LB	MC MC MC MC
U.G. 20 m	CM CM					LB LB	
G G. 31 m	CM CM	M M M M	PM PM				MC MC MC MC
D.T. 17 w			E E S S				
H.K. 30 m	CP CP						

CM Chondromalacia medial condyle
CL Chondromalacia lateral condyle
CL Chondromalacia patellae

M Medial meniscal lesion
L Lateral meniscal lesion

E Effusion
S Synovitis
PM Plica mediopatellaris
PS Plica suprapatellaris

A Rupture of anterior cruciate ligament

OC Osteochondritis dissecans

LB Loose body

MC Medial condyle
LC Lateral condyle
P Patella
C Cyst

References

1. Adam G, Bohndorf K, Prescher A, Krasny R, Günther R W. Der hyaline Gelenkknorpel in der MR-Tomographie des Kniegelenkes bei 1,5 T. Fortschr Röntgenstr 1988; 148(6): 648-51.
2. Adam G, Bohndorf K, Prescher A, Drobnitzky M, Günther R W. Kernspintomographie der Knorpelstrukturen des Kniegelenks mit 3D-Volumen-Imaging in Verbindung mit einem schnellen Bildrechner. Fortschr Röntgenstr 1989; 150(1): 44-8.
3. Aichroth P. Osteochondritis dissecans of the knee. J Bone Joint Surg (Br) 1971; 53, 440.
4. Axhausen G. Über die osteochondritis dissecans Königs. Klin Wschr 1924; 3: 1057-60.
5. Axhausen G. Über den Abgrenzungsvorgang am epiphysären Knochen (Osteochondritis dissecans König). Virchows Arch Path Anat 1924; 252: 458-518.
6. Bellon E M, Keith M W, Coleman P E, Shah Z R. Magnetic resonance imaging of internal derangements of the knee. RadioGraphics 1988; 8(1): 95-118.
7. Beltran J, Noto A M, Herman L J, Mosure J C, Burk J M, Christoforidis A J. Joint Effusions: MR Imaging. Radiology 1986; 158: 133-7.
8. Buckwalter K A, Braunstein E M, Wilson M R, Wojtis E M, Martel W. Evaluation of hyaline cartilage of the knee with MR imaging. Radiology 1986; 161: 239.
9. Burk D L, Kanal E, Brunberg J A, Johnstone G F, Swensen H E, Wolf G. 1.5-T surface-coil MRI of the knee. Amer J Roentgenol 1986; 147,:293-300.
10. Casscells S W. Gross pathological changes in the knee joint of the aged individual. A study of 300 cases. Clin Orthop 1978; 132: 225-32.
11. Clanton T O, DeLee J C. Osteochondritis dissecans. History, pathophysiology and current treatment concepts. Clin Orthop 1982; 167: 50-64.
12. Cotta H, Puhl W, Niethard F U. Der Einflufl des Hämarthros auf den Knorpel der Gelenke. Unfallchirurgie 1982; 8: 148-151.
13. Cox D R, Hinkley D V. Theoretical Statistic. Chapman and Hall, London 1974.
14. Cruess J V. Joint imaging. Diagnostic Radiology. MR Imaging 1988; 175-9.
15. Dexel M, Jehle U. Resultate der operativen Behandlung der Osteochondrosis dissecans am Kniegelenk. Orthopäde 1981; 10: 87-91.
16. Dumas J-M, Edde D J. Meniscal abnormalities: prospective correlation of double-contrast arthrography and arthroscopy. Radiology 1986; 160: 435-56.
17. Engelstad B L, Ramos E C, Johnson T R, White D L, Brasch R C. Development of iron-containing contrast agents. In: Contrast agents in magnetic resonance imaging (Eds. Runge V M, Claussen C, Felix R, James A E). Proceedings of an international workshop, January 1986, San Diego, USA.
18. Ewing J W, Voto S J. Arthroscopic surgical management of osteochondritis dissecans of the knee. Arthroscopy 1988; 4: 37-41.
19. Fassbender H G. Pathologie rheumatischer Erkrankungen. Springer, Berlin-Heidelberg-New York 1975.
20. Ficat P, Hungerford D S. Disorders of the patellofemoral joint. Masson, Paris 1977.
21. Forman M, Muller C, Kayaalp O, Kaplan D. Epidemiology of osteoarthritis of the knee. Arthr and Rheum 1981; Suppl 24: 74 (Abstr. 102).
22. Gadian D G, Payne J A, Bryant D J, Young I R, Carr D H, Bydder G M. Gadolinium-DTPA as a contrast agent in MR imaging—theoretical projections and practical observations. J Computer Assisted Tomography 1985; 9: 242-51.
23. Gallimore G W Jr, Harms S E. Knee injuries: High resolution MR imaging. Radiology 1986; 160: 457-61.
24. Ghelman B. Meniscal tears of the knee: Evaluation by high-resolution CT combined with arthrography. Radiology 1985; 157: 23-7.
25. Green W T, Martin G N, Eanes E D, Sokoloff L. Microradiographic study of the calcified layer of articular cartilage. Arch Path 1970; 90: 151-8.
26. Grodd W, Brasch R C. Magnetopharmazeutische Kontrastveränderungen in der Kernspintomographie. Fortschr Röntgenstr 1986; 145: 130-9.
27. Grueter H, Rütt A. Zur Morphologie der in die Koxarthrose einmündenden Hüftgelenkserkrankungen. Z Orthop 1962; 95: 401-39.
28. Gschwend N, Bischofberger R J. Die Chondropathia patellae. Praxis 1971; 60: 562.
29. Guhl J. Arthroscopic treatment of osteochondritis dissecans. Clin Orthop 1982; 167: 65-74.
30. Gylys-Morin V M, Hajek P C, Sartoris D J, Resnick D. Articular cartilage defects: Detectability in cadaver knees with MR. Amer J Roentgenol 1987; 148: 1153-7.
31. Hajek P C, Sartoris D J, Neumann C, Resnick D. Potential contrast agents for MR arthrography: in vitro evaluation and practical observations. Amer J Roentgenol 1987; 149: 97-104.

32. Hajek P C, Baker L L, Sartoris D J, Neumann C H, Resnick D. MR arthrography: Anatomic-pathologic investigation. Radiology 1987; 163: 141-7.
33. Hajek P C, Sartoris D J, Engel A, Gylys-Morin V, Haghigi P, Kramer F, Resnick D. The effect of intra-articular gadolinium-DTPA on the synovial membrane and cartilage. Investigative Radiology 1990 (in press).
34. Harrison M H M, Schajowicz F, Trueta J. Osteoarthritis of the hip: a study of the nature and evolution of the disease. J Bone Joint Surg (Br) 1953; 35: 598-626.
35. Hartzmann S, Reicher M A, Bassett L W, Duckwiler G R, Mandelbaum B, Gold R H. MR imaging of the knee. Part III. Chronic disorders. Radiology 1987; 162: 553-9.
36. Hnatovich D J, Childs R L, Lateigne D, Najafi A. The preparation of DTPA-coupled antibodies radiolabeled with metallic radionuclides: an improved method. J Immunol Meth 1983; 65: 147-57.
37. Hough A J, Banfield W G, Sokoloff L. Cartilage in hemophilic arthropathy. Arch Path Lab Med 1976; 100: 91-6.
38. Jessar R A. The study of synovial fluid. In: Arthritis and allied conditions (Eds. Hollander J L, McCarty D J), 8th ed. Lea & Febiger, Philadelphia 1976: 67-81.
39. Jonasch E. Das Kniegelenk. Diagnose und Therapie seiner Verletzungen und Erkrankungen. W. de Gruyter, Berlin 1964: 268.
40. Jung T, Rodriguez M, Augustiny N, Friedrich N, von Schulthess G. 1,5-T-MRI, Arthrographie und Arthroskopie in der Evaluation von Knieläsionen. Fortschr Röntgenstr 1988; 148(4): 390-3.
41. Kean D M, et al. Nuclear magnetic resonance imaging of the knee: examples of normal anatomy ond pathology. Brit J Radiol 1983; 56: 355-64.
42. Kirkpatrick C J, Mohr W, Haferkamp O. Alterations in chondrocyte morphology, proliferation and binding of $35SO_4$ due to Fe(III), Fe(II), ferritin and haemoglobin in vitro. Virchovs Arch Zellpath 1982; 38, 297-306.
43. König F. Über freie Körper in den Gelenken. Dt Z Chir 1887; 27: 90.
44. König H, Sauter R, Deimling M, Vogt M. Cartilage disorders: Comparison of Spin-Echo, CHESS, and FLASH sequence MR images. Radiology 1987; 164: 753-8.
45. Köppchen J, Fischer H-J, Becker W, Arnold W, Rietig M. Kernspintomographie von Meniskusläsionen. Z Orthop 1987; 125: 390-5.
46. Köppchen J, Fischer H-J, Becker W, Arnold W. Meniskusdarstellung in der MR-Tomographie mit Oberflächenspulen. Fortschr Röntgenstr 1987; 146(6): 617-22.
47. Lehner K B, Rechl H P, Gmeinwieser J K, Heuck A F, Lukas H P, Kohl H P. Structure, function, and degeneration of bovine hyaline cartilage: assessment with MR imaging in vitro. Radiology 1989; 170: 495-9.
48. Levinsohn E M, Baker B E. Prearthrotomy diagnostic evaluation of the knee: review of 100 cases diagnosed by arthrography and arthroscopy. Amer J Roentgenol 1980; 134: 107-11.
49. Li D, Adams M E, McConkey J P. Magnetic resonance imaging of the ligaments and menisci of the knee. Radiol Clin N Am 1986; 24(2): 209-27.
50. Li K C, Henkelman R M, Poon P Y, Rubenstein J. MR imaging of the normal knee. J Computer Assist Tomography 1984; 6: 1147-54.
51. Middleton W D, Macrander S, Lawson T L, Kneeland J B, Cates J D, Kellman G M, Carrera G F, Foley W D, Jesmanowicz A, Hyde J S. High resolution surface coil magnetic resonance imaging of the joints: Anatomic correlation. Radiographics 1987; 7: 645-83.
52. Mink J H, Reicher M A, Cruess J H. Magnetic resonance imaging of the knee. Raven Press, New York 1987.
53. Mohr W. Gelenkkrankheiten. Diagnostik und Pathogenese makroskopischer und histologischer Strukturveränderungen. Thieme Verlag, Stuttgart, New York 1984: 180, 235-40.
54. Möllmann H, Polster J, Knoche H. Technik der intraartikulären Injektion. Schwarzeck-Verlag, München 1977.
55. Niendorf H P, Seifert W. Serum iron and serum bilirubin after administration of Gd-DTPA-dimeglumine. Invest Radiol 1988; 23(Suppl 1): 275-80.
56. Otte P. Die konservative Behandlung der Hüft- und Kniearthrose und ihre Gefahren. Dtsch Med J 1969; 20: 217-25.
57. Otte P. Synovia und synoviales Milieu im Konzept der aktivierten Arthrose. In: Synovialflüssigkeit und synoviales Milieu (Eds. Thumb N, Kellner G, Klein G, Zeidler H). Symposion Baden bei Wien 1977, Thieme Verlag, Stuttgart, 1979: 3-22.
58. Polly D W, Callaghan J J, Sikes R A, McCabe J M, McMahon K, Savory C G. The accuracy of selective magnetic resonance imaging compared with the findings of arthroscopy of the knee. J Bone Joint Surg (Am) 1988; 70: 192-8.
59. Puhl W, Dustmann H O, Schulitz K-P. Knorpelveränderungen bei experimentellem Hämarthros. Z Orthop 1971; 109: 475-86.
60. Reicher M A, Rauschnig W, Gold R H, Basset L W, Lufkin R B, Glen W. High-resolution magnetic resonance imaging of the knee joint: pathologic correlations. Amer J Roentgenol 1985; 145: 903-9.
61. Reicher M A, Hartzman S, Bassett L W, Mandelbaum B, Duckwiller G, Gold R H. MR imaging of the knee. Part 1. Traumatic disorders. Radiology 1987; 162: 547-51.
62. Reiser M. MRT der Gelenke nach intravenöser und nach intraartikulärer Gabe von Gadolinium-DTPA. In Kontrastmittel für die bildgebende Kernspintomographie 4. Expertengespräch, Bad Rothenfelde 1989.

63. Ribbing S. Zur ätiologie der Osteochondrosis dissecans. Acta Radiol 1944; 25: 732-55.

64. Ropes M W, Bauer W. Synovial fluid changes in joint diseases. Harvard Univ. Press, Cambridge 1953.

65. Schering. Magnevist®, Paramagnetisches Kontrastmittel für die Magnetische Resonanz-Tomographie (MRT). Zeitschrift Diagnostik 5-7, Fa. Schering (edt.) 1988.

66. Schöffler-van der Koelen E, Bezrouk P, Dickmann R. (1979): Über das Vorkommen von Bluteisen in der erkrankten Gelenkkapsel. In: Synovialflüssigkeit und synoviales Milieu (Eds. Thumb N, Kellner G, Klein G, Zeidler H). Symposion Baden bei Wien 1977, Thieme Verlag, Stuttgart 1979: 63-5.

67. Schuler M, Naegele M, Lienmann A, Münch O, Siuda S, Hahn D, Lissner J. Die Wertigkeit der hochauflösenden CT und der Kernspintomographie im Vergleich zu den Standardve rfahren bei der Diagnostik von Meniskusläsionen. Fortschr Röntgenstr 1987; 146(4): 391-7.

68. Selesnick F H, Noble H B, Bachmann D C, Steinberg F L. Internal derangement of the knee: diagnosis by arthrography, arthroscopy, and arthrotomy. Clin Orthop 1985; 198: 26-30.

69. Shahriaree H. Chondromalacia. Contemp Orthop 1985; 11: 27-39.

70. Silva I, Silver D M. Tears of the meniscus as revealed by magnetic resonance imaging. J Bone Joint Surg (Am) 1988; 70: 199-202.

71. Spritzer C E, Vogler J B, Martinez S. MR imagin of the knee: preliminary results with 3DFT GRASS pulse sequence. Amer J Roentgenol 1988; 150: 597-603.

72. Steinbrich W, Beyer B, Friedmann G. MR des Kniegelenkes. Fortschr Röntgenstr 1985; 143: 166-72.

73. Stoller D W, Martin C, Cruess III J V, Kaplan L, Mink J H. Meniscal tears: Pathologic correlation with MR imaging. Radiology 1987; 163: 731-5.

74. Tyrell R L, Gluckert K, Pathria M, Modic M T. Fast three-dimensional MR imaging of the knee: comparison with arthroscopy. Radiology 1988; 166: 865-72.

75. Vilarrubias J M. Handbuch der Infiltrationen im Bewegungsapparat und bei Sportverletzungen. 1. deutschsprachige Auflage, Unas-Verlag, U. Bayer 1987.

76. Vogel H, Krüger L, Hallata Z, Zander C. Knorpel im Kernspintomogramm. Digit Bilddiagn 1986; 6: 118-22.

77. Weinmann H J, Brasch R C, Press W R, Wesby G E. Characteristics of Gadolinium-DTPA complex: a potential NMR contrast agent. Amer J Roentgenol 1984; 142: 619-42.

78. Weinreb J C, Brateman L, Babcock E E, Maravialla K R, Cohen J M, Horner S D. Chemical shift artifact in clinical magnetic resonance imaging at 0.35 T. Amer J Roentgenol 1985; 145: 183-5.

79. Wojtys E, Wilson M, Buckwalter K, Braunstein E, Martel W. Magnetic resonance imaging of knee hyaline cartilage and intraarticular pathology. Amer J Sports Med 1987; 15(5): 455-63.

80. Yulish B S, Montanez J, Goodfellow D B, Bryan P J, Mulopulos G P, Modic M T. Chondromalacia patellae: Assessment with MR imaging. Radiology 1987; 164: 763-6.